



ELSEVIER

Available online at www.sciencedirect.com

SCIENCE @ DIRECT®

MARINE
MICROPALAEONTOLOGY

Marine Micropaleontology 50 (2004) 89–123

www.elsevier.com/locate/marmicro

Reconstructing past planktic foraminiferal habitats using stable isotope data: a case history for Mediterranean sapropel S5

E.J. Rohling^{a,*}, M. Sprovieri^b, T. Cane^c, J.S.L. Casford^d, S. Cooke^e,
I. Bouloubassi^f, K.C. Emeis^g, R. Schiebel^h, M. Rogerson^a, A. Hayesⁱ,
F.J. Jorissen^j, D. Kroon^k

^a School of Ocean and Earth Science, Southampton Oceanography Centre, European Way, Southampton SO14 3ZH, UK

^b Institute for Coastal Marine Environment-CNR, Geomare Section, Calata Porta di Massa, 80, Porto di Napoli, 80100 Naples, Italy

^c School of Chemistry, Physics and Environmental Science, University of Sussex, Falmer, Brighton BN1 9QJ, UK

^d Department of Geography, Science Site, South Road, Durham DH1 3LE, UK

^e Department of Earth Sciences, University of Waikato, Hamilton, New Zealand

^f Laboratoire de Physique et Chimie Marines, Université Pierre et Marie Curie, 4 place Jussieu, 75252 Paris Cedex 05, France

^g Institut für Biogeochemie und Meereschemie, Universität Hamburg, Bundesstr. 55, D-20146 Hamburg, Germany

^h Geological Institute, ETHZ, Sonneggstrasse 5, NOG 32.2, 8092 Zürich, Switzerland

ⁱ Department of Geology, Royal Holloway, University of London, Egham, Surrey TW20 0EX, UK

^j Laboratoire de Géologie, Faculté Sciences, Université d'Angers, 2 Boulevard Lavoisier, 49045 Angers Cedex, France

^k Faculty of Earth Sciences, De Boelelaan 1085, 1081 HV Amsterdam, The Netherlands

Received 16 September 2002; received in revised form 6 June 2003; accepted 14 June 2003

Abstract

A high-resolution stable O and C isotope study is undertaken on all planktic foraminiferal species that are reasonably continuous through an Eemian sapropel S5 from the western side of the eastern Mediterranean. The data are considered within a context of high-resolution isotope records for two further S5 sapropels from the central and easternmost sectors of the basin, alkenone-based sea surface temperature records for all three sapropels, and planktic foraminiferal abundance records for the same sample sets through all three sapropels. Results are compared with similar data for Holocene sapropel S1. The adopted approach allows distinction between species that are most suitable to assess overall changes in the climatic/hydrographic state of the basin, including depth-related differentiations and the main seasonal developments, and species that are most affected by variable biological controls or local/regional and transient physico-chemical forcings. It is found that a-priori assumptions about certain species' palaeohabitats, based on modern habitat observations, may become biased when non-analogue conditions develop. In the case of Mediterranean sapropel S5, these consisted of enhanced freshwater dilution, elevated productivity, shoaling of the pycnocline between intermediate and surface waters, and stagnation of the subsurface circulation. Under these conditions, some species are found to 'shift' into habitat settings that differ considerably from those occupied today. The present multiple-species approach can identify such 'anomalous responses', and thus offers

* Corresponding author. Tel.: +44-1703-593042; Fax: +44-1703-593059.

E-mail address: e.rohling@soc.soton.ac.uk (E.J. Rohling).

a sound background for further shell-chemistry investigations and quantitative interpretation of the isotopic profiles. We capitalise on the latter potential, and offer the first quantitative estimates of monsoon flooding into the Mediterranean during the deposition of Eemian sapropel S5.

© 2003 Elsevier B.V. All rights reserved.

Keywords: planktonic foraminifera; isotopes; Mediterranean; sapropel; palaeohabitats

1. Introduction

Palaeoceanographic interpretations of past planktic foraminiferal assemblages commonly assume that the various species' habitat characteristics in the past were similar to those observed today. Often, a basic distinction is applied between 'mixed-layer' and 'thermocline' dwellers to characterise past water-column gradients and their variability. Some studies go into more detail. Regarding the major species in the Quaternary of the Mediterranean, there has been particular interest in: *Globigerinoides ruber* (w) to reflect summer mixed-layer conditions; *Neogloboquadrina pachyderma* (dextral) as a marker for Intermediate Water shoaling into the base of the euphotic layer, fuelling a distinct Deep Chlorophyll Maximum; and *Globorotalia inflata* and/or *Globorotalia scitula* to reflect the cool, deep, homogeneous and relatively eutrophic winter mixed layer. These habitat characteristics were inferred from habitat studies inside and outside the Mediterranean (e.g. Fairbanks et al., 1982; Hemleben and Spindler, 1983; Thunell and Reynolds, 1984; Bé et al., 1985; Hemleben et al., 1989; Pujol and Vergnaud-Grazzini, 1989; Reynolds and Thunell, 1989; Rohling and Gieskes, 1989; Rohling et al., 1993, 1995; Pujol and Vergnaud-Grazzini, 1995; Reiss et al., 1999; Schiebel and Hemleben, 2000).

The assumption of 'stable' habitat characteristics has developed into an almost fundamental principle to studies that involve chemical analyses of species-specific foraminiferal shells to reconstruct past water-column property gradients (e.g. $\delta^{18}\text{O}$, $\delta^{13}\text{C}$, $\delta^{11}\text{B}$, Mg/Ca, Sr/Ca, Ba/Ca, and Cd/Ca), with increasingly far-reaching interpretations. Oxygen isotope values have been used, after accounting for temperature and ice-volume effects, to estimate past salinities and even palaeo-density gradients (e.g. Thunell and Williams,

1989; Duplessy et al., 1991; Rostek et al., 1993; Maslin et al., 1995; Hemleben et al., 1996; Labeyrie et al., 1996; Kallel et al., 1997a, b). Records of $\delta^{13}\text{C}$, $\delta^{11}\text{B}$, Ba/Ca, and Cd/Ca provide proxies for seawater pH and nutrient concentrations, which in association with other proxy data have been used to reconstruct past pCO₂ and large-scale ocean circulation changes (e.g. Palmer et al., 1998; Pearson and Palmer, 1999, 2000; Boyle and Keigwin, 1982, 1985/86, 1987).

The underlying assumption that habitat characteristics of planktic foraminifera are 'stable' through time remains largely unchallenged. It can be tested by deriving past foraminiferal habitat structures from paired O and C stable isotope analyses. The procedure requires that all (major) species are analysed, and that reasonable – preferably quantitative – concepts and expectations for the analysed signals are developed. We here present a Mediterranean case history along these lines, focussed on the strongly developed anoxic interval known as sapropel S5 in Vicomed core KS205, from the NW Ionian Sea (eastern Mediterranean). S5 dates from the Eemian, Marine Isotope Stage (MIS) 5e, roughly between 124 and 119 ka BP (Cane et al., 2002; Rohling et al., 2002) (Fig. 1). Our work expands on previous studies that pioneered the multiple-species approach in lower resolutions (Ganssen and Troelstra, 1987; Tang and Stott, 1993).

A Mediterranean record is selected because: (1) the modern foraminiferal distribution in this basin is well studied (Pujol and Vergnaud-Grazzini, 1995; Reiss et al., 1999; and references therein); (2) the basin has a relatively small volume and is semi-isolated from the open ocean, so that it shows very rapid and amplified responses to climatic forcings; (3) it is relatively easy to calculate equilibrium calcite $\delta^{18}\text{O}$ values for the various water masses in this basin (e.g. Rohling and De

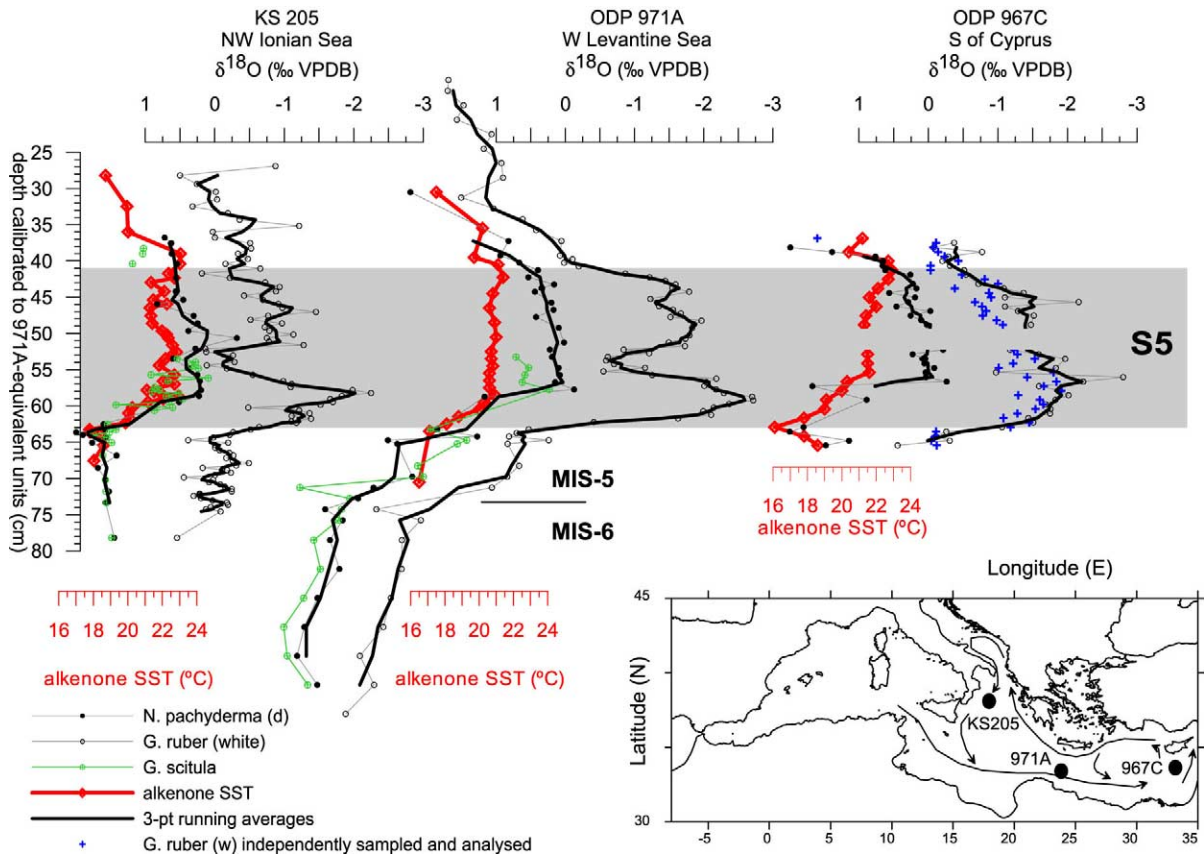


Fig. 1. Summary plot of stable O isotope and alkenone SST records for the three S5 sapropels investigated. The scale of the SST records has been adjusted so that 1°C corresponds with 0.23‰ on the $\delta^{18}\text{O}$ scales (see text) (simplified after Rohling et al., 2002). Development of stratigraphic relationship between the investigated sections and the presence of a small hiatus in S5 of ODP Hole 967C as summarised in the text and extensively discussed in Cane et al. (2002) and Rohling et al. (2002).

Rijk, 1999; Rohling, 1999); (4) there are no problems with diagenetic calcite dissolution or foraminiferal preservation; (5) there is sufficient palaeoceanographic background knowledge to allow the evaluation of new results within a basin-wide context (Fig. 1).

We concentrate on sapropel S5 because the anoxic bottom-water conditions during its deposition prevented bioturbation, so that the resolution of records is constrained only by foraminiferal availability per unit volume of sediment. Also, the Mediterranean circulation regime at times of sapropel deposition was radically different from the present, due to a basin-wide reduction of surface buoyancy loss, while biological productivity was elevated throughout the basin (e.g. Rossig-

nol-Strick et al., 1982; Jenkins and Williams, 1984; Rossignol-Strick, 1983, 1985, 1987; Vergnaud-Grazzini, 1985; Parisi, 1987; Rohling and Gieskes, 1989; De Lange et al., 1990; Rohling and Hilgen, 1991; Castradori, 1993; Rohling et al., 1993, 2000; Rohling, 1994; Thomson et al., 1995; Myers et al., 1998; Cramp and O'Sullivan, 1999; Rohling and De Rijk, 1999; Struck et al., 2001; Casford et al., 2002). The combination of a different circulation regime and elevated productivity offers an ideal 'non-analogue' environment for testing the assumption that habitats remain stable through time.

We present high-resolution stable isotope records for all major planktic foraminiferal species through S5, along with complementing alkenone

sea surface temperature (SST) records. Detailed faunal abundance data on the same samples and the development of a high-resolution (± 1 cm) basin-wide correlation context for S5 may be found in Cane et al. (2002) and Rohling et al. (2002).

The central aims of this study are: to qualitatively and quantitatively assess the habitat characteristics of the investigated species at the time of S5 deposition; to compare those conclusions with the apparent habitats at the time of Holocene sapropel S1 (~ 9 –6 ka BP); and – in particular – to compare the inferred palaeohabitats with the same species' modern observed habitats. This approach identifies which species reflect the general state of circulation, which species are prone to record transient 'anomalies' in the environment and so are of only local relevance, and which species give non-systematic records that contribute little palaeo-environmental understanding. The applied $\delta^{18}\text{O}$ box model further offers new insight into the environmental conditions associated with sapropel S5 – notably the severity of monsoon flooding.

2. Materials and methods

The three S5 sapropels reported here are found at 482.5–506.0 cm in Vicomed core KS205 ($38^{\circ}11.86'\text{N}$; $18^{\circ}08.04'\text{E}$; 2384 m), 40.2–63.0 cm in section 1H-3 of ODP Hole 971A ($24^{\circ}41'\text{N}$; $33^{\circ}43'\text{E}$; 2026 m), and 74.5–103 cm in section 1H-5 of ODP Hole 967C ($34^{\circ}04.27'\text{N}$; $32^{\circ}43.53'\text{E}$; 2554 m) (Fig. 1). A previous correlation study (Cane et al., 2002) allows the records to be plotted with ± 1 cm accuracy along a single depth scale: the 971A-equivalent units (cm) used throughout this paper. Average sediment accumulation rates through the studied sapropels are 4.7, 4.6, and 5.7 cm kyr⁻¹, respectively, based on a 5-kyr duration of S5 deposition (Bar-Matthews et al., 2000; Cane et al., 2002).

S5 presents itself as a dark grey to black sedimentary interval bound by homogeneous pale brown to grey sediments. Persistent bottom-water anoxia during its deposition led to complete absence of benthic foraminifera, starting abruptly at

the onset of the dark colour (Cane et al., 2002). The S5 sapropels in KS205 and 971A were sampled in continuous 0.5-cm intervals. In 967C the interval was 1 cm. Cane et al. (2002) presented full planktic foraminiferal abundance records for all three S5 sapropels along with stable isotope records for *Globigerinoides ruber* (white) and *Neoglobobulimina pachyderma* (dextral). We add records for *Globorotalia scitula* in both 971A and KS205 (Fig. 1), and establish a full-faunal perspective for KS205 by adding data for *Globigerinoides ruber* (pink), *Orbulina universa*, *Globigerinoides sacculifer*, *Globigerinoides sacculifer* (trilobus type), *Globigerinella siphonifera* (wide open-coiled morphotype), *Globigerina bulloides*, *Globigerinita glutinata*, and *Hastigerina pelagica* (Fig. 2). We follow the taxonomic concepts presented by Hemleben et al. (1989) to which we refer for details.

All foraminiferal samples were wet sieved (demineralsed water) into several size fractions, and random splits from the 150–600- μm fraction were used for faunal abundance studies (Cane et al., 2002). The remaining residue was used to pick adult specimens for stable isotope analyses, using a measurement eyepiece to constrain size-windows of ~ 50 μm (abundant species) to ~ 100 μm (rare species) around each species' mean size through the sapropel. Selected specimens were cleaned, where necessary using ultrasound, and dried. The stable isotope analyses were performed on batches of 3–10 specimens, using a PDZ Europa Geo 20–20 mass spectrometer with individual acid-bath carbonate preparation (reaction with orthophosphoric acid at 70°C). Isotope ratios are reported as $\delta^{13}\text{C}$ and $\delta^{18}\text{O}$, in ‰ values relative to Vienna PeeDee Belemnite (VPDB). External precision is better than 0.06 ‰ for both $\delta^{13}\text{C}$ and $\delta^{18}\text{O}$. Any ice-volume effects would equally affect all species investigated, and so cannot account for different trends between species. Comparisons between temperature and $\delta^{18}\text{O}$ values rely on a conversion of 0.23 ‰ °C⁻¹ (O'Neil et al., 1969; Kim and O'Neil, 1997).

For the alkenone SST records, freeze-dried sediments from cores KS205 and 967C were solvent extracted by ultrasonication. Samples from core 971A were extracted in a Dionex ASE 200

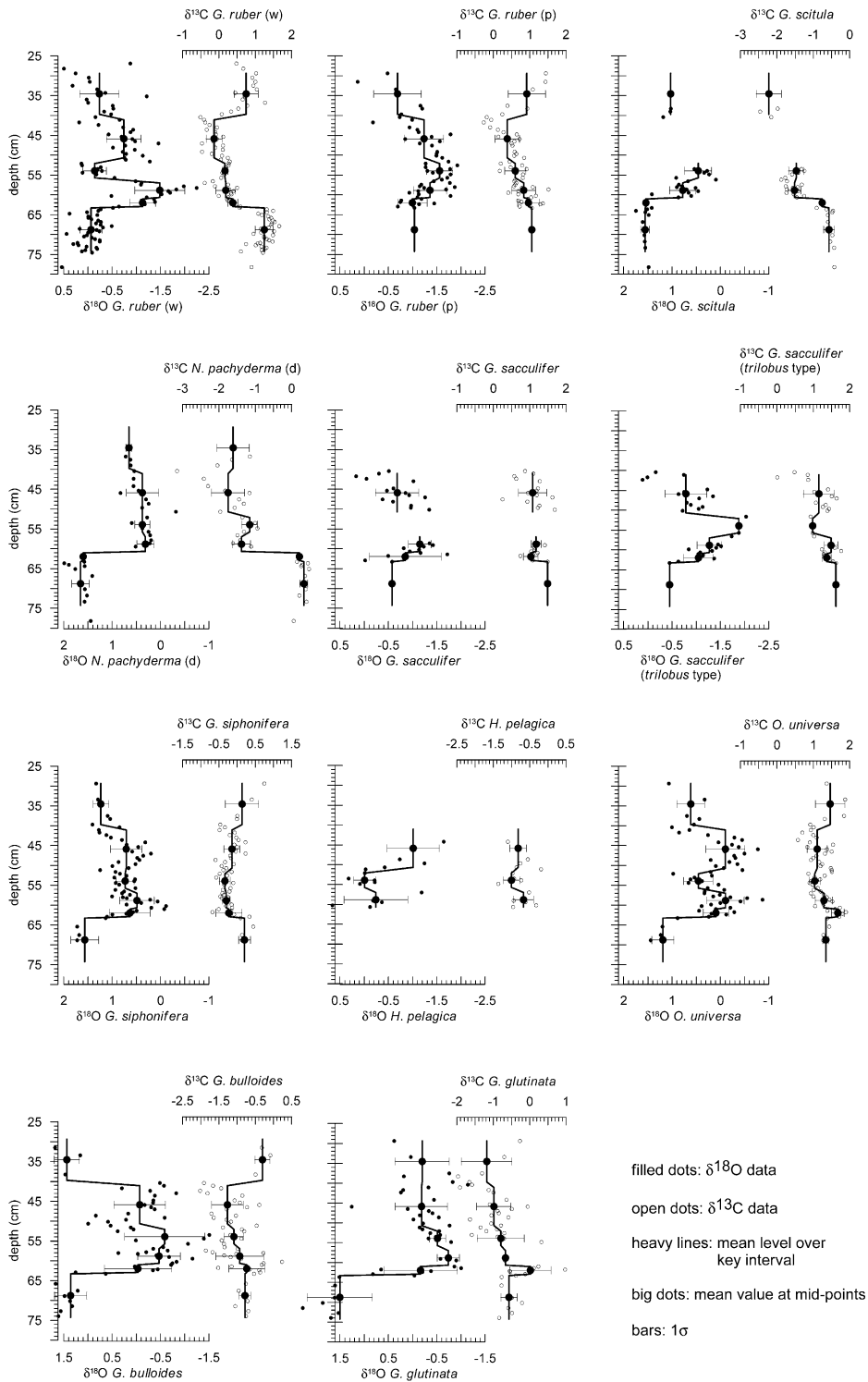


Fig. 2. Side-by-side plots of the $\delta^{18}\text{O}$ and $\delta^{13}\text{C}$ records (in ‰ VPDB) for the various planktic foraminiferal species analysed from S5 in core KS205. Means and standard deviations are shown for the various intervals through S5 identified in Table 2a,b.

Accelerated Solvent Extractor after adding 1 μg cholestane and *n*-C₃₆, and 0.5 μg nonadecanone as internal standards (extraction pressure N₂ 80 bar, temperature 75°C, solvent 100% dichloromethane). Extraction vessels were packed at base with 2 cm extraction-grade silica gel (modified diatomaceous earth). Alkenone fractions were isolated by silica gel column chromatography (core KS205), or by high pressure liquid chromatography (HPLC) (core 967C), and analysed by capillary gas chromatography (GC). Extracts from core 971A were analysed without prior clean up. Alkenones were identified based on their retention times and those of standards. The alkenone unsaturation index $U_{37}^k = C_{37:2}/(C_{37:2} + C_{37:3})$ was calculated from peak areas and translated into temperatures using the global calibration derived by Müller et al. (1998): $\text{SST } (^{\circ}\text{C}) = (U_{37}^k - 0.044)/0.033$. Emeis et al. (1998; 2000) and Rohling et al. (2002) provide further details on the alkenone SST determinations and the calibration.

The temporal resolution in the analytical series through S5 for *Globigerinoides ruber* (w), *G. ruber* (p), *Globigerinella siphonifera*, *Orbulina universa*, and *Globigerina bulloides* is ~ 100 years for an S5 duration of ~ 5 kyr. Results for *Neogloboquadrina pachyderma*, *Globorotalia scitula*, *Globigerinoides sacculifer* (with sac-like final chamber), *G. sacculifer* (trilobus type), *Globigerinita glutinata*, and *Hastigerina pelagica* are wider spaced, limited by variations in the availability of suitable specimens (Fig. 2). The alkenone SST record for S5 in KS205 has an average temporal resolution of ~ 160 years. Note that the applied 5-kyr duration for S5 substantially exceeds the radiocarbon dated 3 kyr for Holocene sapropel S1 (Stanley and Maldonado, 1979; Vergnaud-Grazzini, 1985; Troelstra et al., 1991; Jorissen et al., 1993; Mercone et al., 2000).

3. Concept/working hypothesis

3.1. Identifying water masses

The warm summer mixed layer is thinner, hence less voluminous, than the deep and cool winter mixed layer. Any runoff event or heating anomaly

would therefore leave a signal of considerably larger magnitude in summer than a similar-scale event in winter. The effects of a runoff event would be particularly noticeable in a thin layer or lenses, stabilised at the surface by a transient halocline. Considerable $\delta^{18}\text{O}$ variability is therefore expected in the summer mixed layer, and especially in association with any narrow top-layers/lenses. In the Mediterranean, such lenses are expected due to the seasonal monsoon flooding (today concentrated via the Nile), which peaks in NE Africa over a period of ~ 2 months centred on August (Maynard et al., 2002). In freshwater-diluted layers/lenses, the low freshwater $\delta^{18}\text{O}$ anomaly remains concentrated until the halocline breaks down and the anomaly gets mixed through the more extensive mixed layer. Lenses of freshwater-diluted mixed-layer water are known to survive for extended periods of time and large distances with distinct nutrient/mixing characteristics, creating potential habitats that differ greatly from those in adjacent surface waters (e.g. Zaire and Amazon/Orinoco plumes: Ryther et al., 1967; Calef and Grice, 1967; Nof, 1981; Ufkes et al., 1998; Schmuker, 2000; Schmuker and Schiebel, 2002). Concerning stable carbon isotopes, the summer mixed layer should theoretically show the heaviest (most ^{13}C enriched) $\delta^{13}\text{C}$ values in the water column, as ^{12}C is preferentially sequestered during photosynthesis within the euphotic layer and removed from the surface layers by export production ('biological pump'). If extensive freshwater addition takes place, however, surface waters could record ^{12}C enrichment: freshwater not only contains dissolved inorganic carbon with $\delta^{13}\text{C}$ values of -5 to -10‰ , but in addition carries dissolved and suspended organic carbon (e.g. humics) with $\delta^{13}\text{C}$ values as low as -27‰ (Fontugne and Calvert, 1992).

Waters below the summer mixed layer, i.e. below the seasonal thermocline, are very similar in temperature (*T*) and salinity (*S*) to the winter mixed layer, since the summer mixed layer 'grows' in the previous winter mixed layer by warming progressively from the surface downwards, aided by reduced wind-driven mixing in the calmer summer season. The subthermocline part of the

surface system in summer therefore remains dominated by winter-typical properties. These winter-typical properties evolve in the deep winter mixed layer, whose great homogenised volume restricts the amplitude of isotopic anomalies in response to hydrological events. The $\delta^{18}\text{O}_{\text{calcite}}$ records for winter-type waters will therefore be characterised by reduced variability and, due to the lower temperatures, by a distinct offset to heavier values relative to $\delta^{18}\text{O}_{\text{calcite}}$ records for the summer mixed layer.

The relatively shallow (150–600 m) intermediate waters in the eastern Mediterranean in essence represent winter waters from the region with highest surface densities. Today, this condition is achieved between Cyprus and Rhodes (e.g. Wüst, 1961; POEM group, 1992; Roether and Well, 2001), and at times of sapropel formation it likely occurred in the Adriatic Sea (Myers et al., 1998; Rohling et al., 2000; Casford et al., 2002). Away from those areas, therefore, the intermediate water reflects a long-term mixture of intense winter conditions in a relatively remote region, which would by virtue of long-term (decadal-scale) homogenisation have lost almost all short-term variability in T , S , and $\delta^{18}\text{O}$. Basically, it acts like a giant capacitor that eliminates high-frequency noise, generating a stable long-term averaged signal.

Records of $\delta^{18}\text{O}_{\text{calcite}}$ cannot further distinguish between the main winter-water types (winter mixed-layer, summer subthermocline, and intermediate waters), except possibly for heavier mean values in species living in the somewhat colder and/or more evaporated intermediate water. Helpful contrasts are expected in the $\delta^{13}\text{C}_{\text{calcite}}$ records. While both the summer and winter mixed layers equilibrate with the atmo-

sphere, the summer subthermocline (winter-type) waters remain seasonally isolated, awaiting the next deep winter mixing and building up a ^{12}C excess due to respiration. The resultant (light) $\delta^{13}\text{C}$ anomaly depends on the vigour of export production and respiration. However, it would remain smaller than the anomaly in the intermediate water: the relatively remote nature of the intermediate water, combined with its depth range that coincides with the mid-depth remineralisation maximum, determines that it becomes even more enriched in respiration products (cf. Pierre, 1999). Today, with very active intermediate water ventilation and oligotrophic conditions throughout the eastern Mediterranean, the surface to intermediate water $\delta^{13}\text{C}_{\Sigma\text{CO}_2}$ gradient in the western Levantine and Ionian Basins is typically of the order of 0.3‰ (Pierre, 1999). It would be enhanced at times with elevated productivity and reduced ventilation.

The above suggests that the O and C isotope ratios in the various planktic foraminiferal species should distinguish up to five different water masses in the upper water column (Table 1). Specimens living in or very near to the thin top-layer/lenses of warm surface waters affected by freshwater floods from the (late) summer monsoon will display light and highly variable $\delta^{18}\text{O}$ values, along with variable $\delta^{13}\text{C}$ compositions between rather heavy (productivity effect) and very light values (terrestrial carbon influence). Those living in the more extensive warm summer mixed layer can be distinguished on the basis of light $\delta^{18}\text{O}$ values, although not as light and variable as those in the thin freshwater-affected layer, and less variable and likely heavier $\delta^{13}\text{C}$ values. Specimens living in cold winter-type waters will display $\delta^{18}\text{O}$ records with generally heavy mean

Table 1

Schematic presentation of $\delta^{18}\text{O}$ and $\delta^{13}\text{C}$ trends expected in equilibrium calcite precipitated within the various Mediterranean surface to intermediate water masses, as discussed in the text, along with their expected variability (more dots = higher variability)

	$\delta^{18}\text{O}$	$\delta^{18}\text{O}$ variability	$\delta^{13}\text{C}$	$\delta^{13}\text{C}$ variability
Fresh top-layer/lenses	--	●●●●	- to ○	●●●
Summer mixed layer	-	●●●	○ to ++	●
Summer subthermocline	+	●●	- to --	●●
Winter mixed layer	+	●●	- to +	●
Intermediate water	++	●	---	●●●

values and suppressed variability. Those from the winter mixed layer proper will combine these characteristics with rather constant $\delta^{13}\text{C}$ values, although light values may be introduced when deep turbulence ‘erodes’ the underlying nutricline.

Foraminifera from summer subthermocline waters are likely to record winter-type $\delta^{18}\text{O}$ values combined with light $\delta^{13}\text{C}$ values. Specimens from intermediate waters are likely to record winter-type $\delta^{18}\text{O}$ values (possibly somewhat heavier and

Table 2a

Reported deviations from $\delta^{18}\text{O}$ of *Globigerinoides ruber* or $\delta^{18}\text{O}_{\text{equilibrium calcite}}$

Species	Temperature (°C)			Source	Location
	15.0	20.0	25.0		
<i>G. ruber</i>	−0.02	−1.06	−2.10	Spero et al., 2003	Culture
Deviations from $\delta^{18}\text{O}_{G. ruber}$ (values shown are $\delta^{18}\text{O}_{\text{species}} - \delta^{18}\text{O}_{\text{ruber}}$ ‰)vpdb)					
<i>G. sacculifer</i> ^a (> 650µm)	−0.51	−0.35		Spero et al., 2003	Culture
<i>G. menardii</i>	0.00	0.07	0.13	Mielke, 2001	Culture
<i>N. dutertrei</i>	−0.61	−0.38	−0.05	Bouvier-Soumagnac and Duplessy, 1985	Plankton tow in Indian Ocean
<i>G. bulloides</i> (11 chambered)	−0.45	−0.40	−0.34	Bemis et al., 1998	Culture
<i>G. bulloides</i> (12 chambered)	−0.35	−0.33	−0.31	Bemis et al., 1998	Culture
<i>G. bulloides</i> (13 chambered)	−0.27	−0.28	−0.29	Bemis et al., 1998	Culture
<i>O. universa</i> (low light)	0.33	0.33	0.33	Bemis et al., 1998	Culture
<i>O. universa</i> (high light)	0.00	0.00	0.00	Bemis et al., 1998	Culture
<i>N. pachyderma</i>	0.40	0.62	0.84	von Langen et al., 2000	Culture
Deviations from $\delta^{18}\text{O}_{\text{equilibrium calcite}}$ for deep dwelling species at ~6°C					
<i>G. scitula</i>		−0.4		Ortiz et al., 1996	Plankton tow in northeastern Pacific
<i>G. hexagona</i>		−0.4		Ortiz et al., 1996	Plankton tow in northeastern Pacific
<i>N. pachyderma</i> (s) ^b		−1		Bauch and Wefer, 1997	Plankton tow in Arctic Ocean
<i>N. pachyderma</i> (s) ^b		−0.9 to −1.0		Simstich et al., 2003	Plankton tow in Nordic Seas
<i>N. pachyderma</i> (s) ^b		−0.7		Ortiz et al., 1996	Plankton tow in northeastern Pacific
<i>G. calida</i> ^{2b}		−0.6		Ortiz et al., 1996	Plankton tow in northeastern Pacific
Deviations from $\delta^{18}\text{O}_{\text{equilibrium calcite}}$ from a plankton tow near Bermuda ^c					
	Mean	St. dev.			
<i>G. ruber</i> (white)	−2.03	0.70		Williams et al., 1981	Plankton tow near Bermuda
<i>G. ruber</i> (pink)	−2.28	0.19		Williams et al., 1981	Plankton tow near Bermuda
<i>G. conglobatus</i>	−2.03	0.16		Williams et al., 1981	Plankton tow near Bermuda
<i>G. siphonifera</i>	−0.55	0.76		Williams et al., 1981	Plankton tow near Bermuda
<i>G. truncatulinoides</i>	−1.04	0.17		Williams et al., 1981	Plankton tow near Bermuda
<i>G. hirsuta</i> ^d	−1.05	0.01		Williams et al., 1981	Plankton tow near Bermuda

For *G. ruber*, the deviation given is relative to equilibrium, which is dependent on temperature according to $T(^{\circ}\text{C}) = 1.49 - 4.8(\delta^{18}\text{O}_{\text{ruber}} - \delta^{18}\text{O}_{\text{equilibrium calcite}})$ (requires local calibration (Spero et al., 2003)).

^a Deviation dependent on test size and on light influence. Individuals taken from 250–350µm fraction are offset by ~0.3‰ (Spero et al., 2003).

^b Relative to dwelling depth (may calcify at shallower depths (Ortiz et al., 1996)).

^c Size (140–510µm) and temperature (27.6–19.4°C) are variable (Williams et al., 1981).

^d Only two data points are available for *G. hirsuta*

Table 2b

Deviation from $\delta^{13}\text{C}_{\text{DIC}}$ varies as a function of the equation: $\delta^{13}\text{C}_{\text{DIC}} = \delta^{13}\text{C}_s + \Delta\delta^{13}\text{C}_o Q_{10}^{(T-T_0)/10}$ where Q_{10} is the change in metabolic rate over a change of 10°C (not constant over broad temperature changes and requires local calibration) (Ortiz et al., 1996).

Species	Deviation from DIC	Source	Location
<i>G. ruber</i>	+0.94	Bemis et al., 1998	Culture
<i>G. sacculifer</i> (>650 μm)	-0.73	Spero et al., 2003	Culture
<i>G. sacculifer</i> (250–350 μm)	+0.19		
<i>G. menardii</i>	0.00	Mielke, 2001	Culture
<i>N. dutertrei</i>	-0.50	Bouvier-Soumagnac and Duplessy, 1985	Plankton tow in Indian Ocean
<i>G. bulloides</i> ^a	-3.65	Bemis et al., 2000	Culture
<i>O. universa</i> (low light)	-1.20	Bemis et al., 1998	Culture
<i>O. universa</i> (high light)	-0.30	Bemis et al., 1998	Culture
<i>G. scitula</i>	-1.1	Ortiz et al., 1996	Plankton tow in northeastern Pacific
<i>G. hexagona</i>	-0.8	Ortiz et al., 1996	Plankton tow in northeastern Pacific
<i>N. pachyderma</i> (sinistral) ^b	-0.75	Ortiz et al., 1996	Plankton tow in northeastern Pacific
<i>G. calida</i> ^b	-0.25	Ortiz et al., 1996	Plankton tow in northeastern Pacific

^a Dependent on size.

^b Relative to dwelling depth (may calcify at shallower depths (Ortiz et al., 1996)).

with less short-term variability) accompanied by the lightest $\delta^{13}\text{C}$ values.

Finally, some species may show very little systematic behaviour in their $\delta^{18}\text{O}$ and $\delta^{13}\text{C}$ records. This would be characteristic of species that live by preference during seasonal ‘transitions’ of intensive mixing (e.g. the autumn breakdown of stratification) or early water-mass separation (e.g. spring build-up of seasonal stratification). Considering the ‘identified’ water masses as ‘mixing end-members’, such species would be expected to show strong variability between the end-member extremes. Another possible cause for non-systematic behaviour in foraminiferal $\delta^{18}\text{O}$ and $\delta^{13}\text{C}$ records relates to the unknown potential of the various species to experience a shift of their optimum shell-production conditions through the seasonal cycle, or in the vertical through the water column, in response to changes in overlooked (biological?) controls on their abundance distribution. One would then expect inexplicable variability independent of other signals when viewed over the whole record, although it may covary with other signals over parts of the record.

3.2. Vital effects

Most species secrete their calcite tests out of isotopic equilibrium for $\delta^{18}\text{O}$ and $\delta^{13}\text{C}$, due to

so-called ‘vital effects’ (Table 2a,b) (e.g. Williams et al., 1981; Bouvier-Soumagnac and Duplessy, 1985; Spero and Williams, 1988; Ortiz et al., 1996; Bemis et al., 1998; Peeters, 2000; Simstich et al., 2003; Spero et al., 2003). General overviews can be found in Grossman (1987), Ravelo and Fairbanks (1995), Spero et al. (1991), and Rohling and Cooke (1999). Palaeoceanographic studies allow for such processes by considering that the vital-effect offset from equilibrium is a constant through time for each species. The relative trends and variability in isotopic records are independent of such systematic disequilibria, which only affect the absolute values.

There is no a-priori ‘correction’ for vital effect offsets in this study, because no values are yet available for specimens originating from the Mediterranean. In view of the extensive genetic differentiation within planktonic foraminiferal morphospecies (e.g. Darling et al., 2000; Stewart et al., 2001; Kucera and Darling, 2002; Pawlowski and Holzmann, 2002), we consider that the Mediterranean’s quasi-isolation over at least 5 million years may well have fostered a fauna of endemic genotypes with vital-effect offsets that differ from those in their open oceanic morphological counterparts. In view of this uncertainty, it is more sensible to work with actually measured values than with values derived from a potentially erro-

neous ‘correction’. For completeness, the most commonly reported (extra-Mediterranean) vital-effect values are listed in [Table 2a,b](#). Note that this table illustrates that straightforward ‘corrections’ would also be difficult: (a) because the offsets for several of the species investigated here have not yet been determined; and (b) since – when determined – the offsets appear to be sensitive to SST. Our stable oxygen isotope model offers some crude insight into (dis-)equilibrium values of the various species within the Mediterranean setting, for comparison with values in [Table 2a,b](#).

3.3. *Modelling $\delta^{18}O$ variations*

The implications for $\delta^{18}O$ of equilibrium calcite within the water masses discussed above are modelled using a previous Mediterranean $\delta^{18}O$ box model ([Rohling, 1999](#)). It is modified by separation of its single surface box into a succession of a winter mixed-layer box, a summer mixed-layer box, a summer-subthermocline box, and a monsoon-affected top-layer box within the summer mixed layer ([Fig. 3](#)). It calculates $\delta^{18}O_{\text{water}}$, salinity, and $\delta^{18}O_{\text{calcite}}$ for the various end-member water masses. Values of $\delta^{18}O_{\text{calcite}}$ in between those of the end-members may result from (a) mixtures between end-member water masses, or

(b) initial stages of temperature change. An example of (a) would be a partial breakdown of the halocline that separates freshwater lenses (monsoon box) from the rest of the summer mixed layer. The $\delta^{18}O$ signals of foraminifera secreting shells under such conditions would score in between the values calculated for the monsoon box and the summer mixed-layer box. An example of (b) concerns the initial warming in the winter mixed layer at the early stages of seasonal stratification in spring. The $\delta^{18}O$ values of foraminifera living under such conditions would range in between those modelled for the winter mixed-layer box and the summer mixed-layer box.

The model contains a primitive annual cycle that consists of a 6-month summer and a 6-month winter. Precipitation onto the sea at any time is taken according to its present-day proportion relative to evaporation (40%: [Garrett et al., 1993](#)). The portion of runoff that equals the present-day runoff into the basin (‘normal’ runoff) is apportioned equally over the year. During periods of sapropel formation, late summer monsoon-sourced runoff into the basin was strongly enhanced ([Adamson et al., 1980](#); [Rossignol-Strick et al., 1982](#); [Rossignol-Strick, 1983, 1985, 1987](#); [Rohling et al., 2002](#)). This influence is approximated by imposing a monsoon-affected box at the very surface of the summer mixed layer

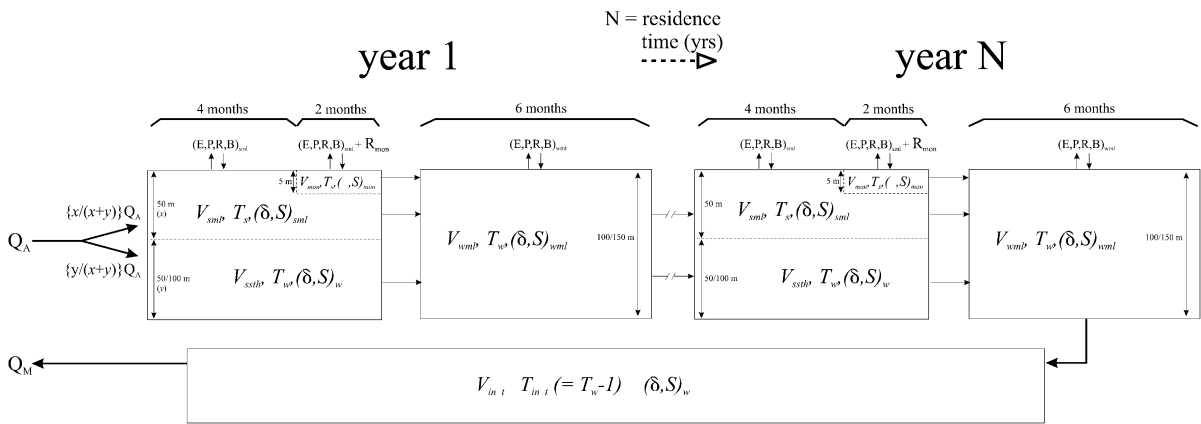


Fig. 3. Schematic representation of the model used to calculate property changes in the various surface and intermediate water masses. *V* stands for volume, *T* for temperature, δ for $\delta^{18}O$, *S* for salinity, *E* for evaporation, *P* for precipitation (onto sea), *R* for runoff, *B* for Black Sea influence (treated in analogy the present, as part of *R*; cf. [Rohling, 1999](#)), and *Q* for the exchange fluxes through the Strait of Gibraltar. The model resolves for the residence time of water in the boxes, and iteratively solves the property changes for the appropriate (integer) number of years.

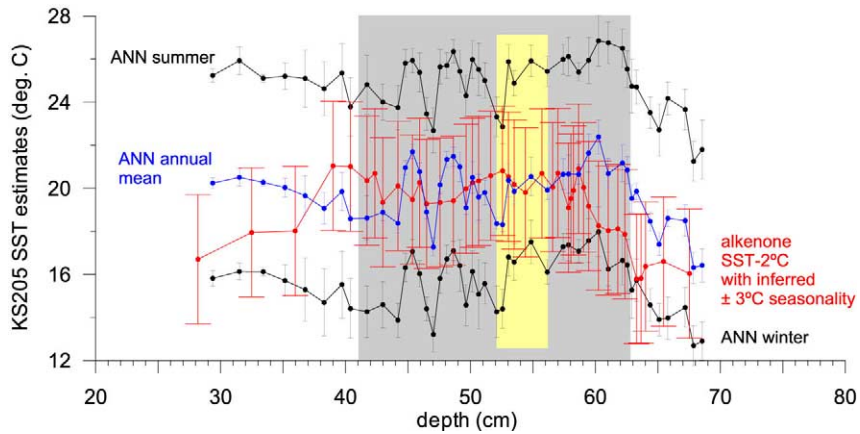


Fig. 4. Comparison between the alkenone-based mean SST and seasonal range (red bars) used in the oxygen isotope model, and the annual mean (blue) and summer+winter SST (black) values obtained from the preliminary application of the Artificial Neural Network method for deriving Mediterranean SST (Hayes et al., 2003). ANN values reported with 1σ uncertainty limits.

over a period of two months. This box is assigned a depth of 5 m over the entire basin, to primitively simulate considerably diluted conditions in response to the monsoon flooding, which in reality would be found concentrated in lenses or patches. This simplification is justified as we only aim to approximate relationships between the main trends in the various $\delta^{18}\text{O}$ records, not to realistically simulate circulation, and it is evaluated using sensitivity tests. The monsoon box allows assessment of the potential affinity of foraminiferal species with freshwater-diluted layers/lenses.

Inflow into the Mediterranean is regulated using a simplified version of the Bryden and Kinder (1991) model for exchange transport through the Strait of Gibraltar (cf. Rohling, 1999). Sea level for the time of S5 is taken constant and similar to the present, so that exchange transport through the Strait of Gibraltar only depends on changes in excess evaporation, according to $Q_A/Q_A^p = (X/X^p)^{1/3}$ where Q_A is the inflow from the Atlantic into the Mediterranean, X is excess of evaporation over total freshwater influx, and p indicates present-day values. Inflow is proportionally separated into the mixed-layer and subthermocline boxes according to the thickness of these boxes relative to the total surface-system depth. For non-sapropel times, the total surface-system depth is taken as 150 m, which then equals the total

depth of the winter mixed layer, and which in summer separates into a 50-m mixed-layer box and a 100-m-thick subthermocline box. A basin-wide shoaling of the interface between surface and intermediate waters is well-documented for times of sapropel formation (Rohling and Gieskes, 1989; Castradori, 1993; Rohling, 1994; Myers et al., 1998). Consequently, the surface system for those times is set to a (winter mixed-layer) depth of 100 m, which in summer separates into 50 m for the mixed layer box and 50 m for the subthermocline box.

The hydrological cycle affects boxes exposed at the surface. Evaporation is calculated as outlined in Rohling (1999) with respect to the temperature of the box exposed at the surface (T_s for the summer mixed-layer and monsoon boxes, T_w for the winter mixed-layer box). Relative humidity, sea-air temperature contrast, and wind speed are kept constant at annual mean values of 70%, 0.5°C and 7.5 m s^{-1} (cf. Rohling, 1999). Seasonal temperatures are calculated using alkenone SSTs as an approximation of annual average SST (Rohling et al., 2002), and allowing seasonal deviations from the mean of $+3^\circ\text{C}$ in summer to -3°C in winter (Stanev et al., 1989). Since the alkenone SSTs are determined for the eastern Mediterranean, whereas the model concerns the entire basin, alkenone SSTs were first adjusted by -2°C to compensate for the difference between

mean SST in the eastern basin only and mean SST in the entire Mediterranean.

We have performed preliminary SST reconstructions using an Artificial Neural Network approach (Hayes et al., 2003) on the planktonic foraminiferal abundance data through S5 in core KS205 as given in Cane et al. (2002). The results broadly corroborate the schematic mean and seasonal change in SST used in the model calculations, although we may be underestimating seasonal variability by up to 2°C (Fig. 4). It also appears that the fauna-based SST values are considerably higher than the alkenone-based estimates in the ‘pre-S5’ and ‘base lower lobe’ intervals (cf. Table 3), suggesting that our derived monsoon flooding values for that interval could be exaggerated and in fact may have been more similar to those in the ‘upper lobe’ of S5. It remains to be established whether the difference in SST estimates reflects a change in the dominant bloom season of alkenone producing phytoplankton, or some problem with the ANN method like a productivity overprint. Inductively Coupled Plasma–Atomic Emission Spectroscopy (ICP–AES) based Mg/Ca analyses on foraminiferal calcite from S5 in KS205 (*Globigerinoides ruber* w and *Neogloboquadrina pachyderma* d) proved inconclusive because of erratic large-amplitude variability in the ratios (between 2 and 8 mmol/mol). Similarly erratic results were obtained from benthic foraminiferal calcite from eastern Mediterranean sapropel S1, using laser-sampling ICP–MS (Reichert, pers. commun., Nice, April 2003).

The model calculates mean residence times in the surface system and then iterates over the ap-

propriate number of annual cycles (Fig. 3). Winter mixing homogenises all summer boxes over the entire depth of the surface system (150 m in non-sapropel times, 100 m in sapropel times). Winter evaporation is calculated at temperature T_w . Precipitation is taken at 40% of evaporation, and runoff into the (6-month) winter mixed-layer box is $6/12$ of the ‘normal’ (= present-day) annual runoff. Next, the surface-most 50 m is separated (summer mixed layer). It undergoes evaporation at temperature T_s and receives a proportional amount (40%) of precipitation. The summer mixed-layer box is exposed to the hydrological cycle for 4 months, and so receives $4/12$ of the annual ‘normal’ runoff. The summer subthermocline box, which makes up the rest of the total depth of the surface system (50–150 m in non-sapropel times and 50–100 m in sapropel times), is not exposed and ‘preserves’ the properties achieved at the end of the previous winter mixed-layer episode. During two months at the end of summer in periods with specified monsoon intensification (Table 3), a 5-m-thick layer is separated from the summer mixed-layer box at the very surface, to form the ‘monsoon box’. Over these two months, the monsoon box sustains the effects of evaporation (at T_s), and receives a proportional amount of precipitation as well as $2/12$ of the ‘normal’ annual runoff. The monsoon box also receives the entire excess monsoon flooding imposed on the model. Monsoon intensification is quantified by a ratio, M , between the volume of the monsoon flood and that of the annual ‘normal’ (= present-day) runoff. A new ‘year’ is started in the model’s iterative sequence with the

Table 3
Model parameters used in the main run discussed in the present paper

Plot depth (cm)	Interval	Monsoon intensification factor (M)	Monsoon box	Interface shoaling ^a	T_s^b (°C)	T_w^b (°C)
39.71–29.37	Post S5	0	N	N	21.4	15.4
50.65–41.06	Upper ‘lobe’	2	Y	Y	22.9	16.9
55.72–52.10	Interval	0	N	Y	23.4	17.4
60.64–57.00	Top lower lobe	3	Y	Y	22.7	16.7
62.92–61.03	Base lower lobe	3	Y	Y	21.0	15.0
74.24–63.29	Pre S5	0	N	N	19.1	13.1

^a Concerns the intermediate to surface water interface. If shoaling is applied (periods of sapropel formation, see text), the total depth of the surface system in the model is set to 100 m, vs. 150 m where no shoaling is applied.

^b Temperatures derived from the mean values for the identified intervals in the alkenone SST record, as explained in the text.

homogenisation of all water masses to give the next winter's mixed-layer conditions. After completion of the iterative sequence, the final salinity and $\delta^{18}\text{O}$ values are noted for all boxes. End-product winter waters are used to represent the properties of intermediate water, which sustains the outflow from the basin through the Strait of Gibraltar (Fig. 3).

Environmental controls on $\delta^{18}\text{O}$ in the various boxes are treated as in Rohling (1999), except that we here keep the $\delta^{18}\text{O}$ of 'normal' runoff continuously at -6‰ , rather than variable between -6‰ (non-sapropel times) and -8‰ (sapropel times) as in the earlier study. The present model allows the monsoon floods to enter the 2-month monsoon box with isotopic values between -8 and -10‰ , in agreement with the isotopic conditions reconstructed for monsoon floods (Sonn-tag et al., 1979; McKenzie, 1993; Rozanski, 1985; Hoelzmann et al., 2000; Gasse, 2000).

After determination of salinity and $\delta^{18}\text{O}_{\text{water}}$ in all boxes, the appropriate temperature for each box (T_s or T_w) is used to calculate equilibrium calcite $\delta^{18}\text{O}_{\text{calcite}}$ by means of the equations of O'Neil et al., 1969; Coplen et al. (1983), and NIST (1992) (see elaboration in Rohling, 1999). The $\delta^{18}\text{O}_{\text{calcite}}$ value for intermediate waters considers an extra 1°C cooling. Although a rough approximation, this gives a useful confidence margin to the identification of species that reflect extreme winter-water conditions.

4. Results and discussion

4.1. Qualitative habitat assessment

The isotope results for S5 in KS205 are consistent with those for S5 in ODP 971A and in ODP 967C (Fig. 1). The alkenone SST records show stable high values through all three S5 sapropels, although the high 'plateau' is reached considerably after the onset of the sapropel (Fig. 1). The $\delta^{18}\text{O}_{G. ruber (w)}$ records of KS205 and 971A show a general shift to light values within S5 that is interrupted by a brief enrichment. Neither of the two independently sampled and analysed $\delta^{18}\text{O}_{G. ruber (w)}$ records for 967C shows this 'inter-

ruption'. Overall, the lightest $\delta^{18}\text{O}_{G. ruber (w)}$ values are found in 971A (Fig. 1), similar to observations of lightest $\delta^{18}\text{O}$ values in the easternmost Ionian Sea/westernmost Levantine Sea for other sapropels (Fontugne et al., 1994; Emeis et al., 2003). The implications of this spatial $\delta^{18}\text{O}$ distribution pattern were elaborated previously (Rohling et al., 2002). Here, we emphasise that, despite local/regional differences, the general faunal and isotope patterns in KS205 are representative of S5 on a basin-wide scale (see also Corselli et al., 2002).

Figs. 2 and 5 present the isotope data through S5 in core KS205, along with means and $\pm 1\sigma$ bounds for six key intervals (means for S5 as a whole are listed in Table 4). The key intervals (Table 3) have been selected to capture the main 'states' in the records, avoiding the inclusion of strong shifts. The alkenone SST data are presented in Fig. 1, and means and $\pm 1\sigma$ bounds for the KS205 alkenone SST values in the six key intervals are shown in Fig. 5, after conversion to equivalent shifts in equilibrium calcite $\delta^{18}\text{O}$.

We are primarily concerned with differences between the general trends (mean values) in the various species' $\delta^{18}\text{O}$ records, and also consider the level of short-term variability/noise around those trends. The $\delta^{18}\text{O}$ signals of *Globorotalia scitula* and *Neogloboquadrina pachyderma* (d) are very stable, with little short-term variability (Fig. 2). In fact, changes in $\delta^{18}\text{O}_{N. pachyderma}$ (d) and $\delta^{18}\text{O}_{G. scitula}$ are so limited to general trends that they show a highly significant positive covariation with one another from the top of MIS-6 through S5 ($N=36$; $R^2=0.92$; $\delta^{18}\text{O}_{G. scitula}=0.85\delta^{18}\text{O}_{N. pachyderma}+0.39$). In view of the statistical nature of specimen selection for isotope analysis, one would expect considerable 'random' variability between individual analyses, and especially between series for two different species, unless these species (a) derived from a water mass with remarkable stability, displaying only long-term trends and no short-term 'noise', and (b) strictly adhered to one and the same, narrowly-constrained habitat. We also note that the $\delta^{18}\text{O}_{G. scitula}$ and $\delta^{18}\text{O}_{N. pachyderma}$ (d) data show a significant positive correlation with the alkenone SST estimates ($N=16$; $R^2=0.42$, and $N=19$;

$R^2 = 0.67$, respectively). This suggests a close adherence to the general temperature developments in the basin with little interference from short-term environmental variability, which again implies a habitat in a water mass with remarkable temporal stability.

The $\delta^{18}\text{O}$ records of *Globigerinoides ruber* (w), *G. ruber* (p), *Globigerinita glutinata*, *Orbulina universa*, and *Globigerinoides sacculifer* (*trilobus* type) instead show strong short-term variability around the mean trends, and no significant relationship with the alkenone SST trends (Fig. 2). Since the actual $\delta^{18}\text{O}$ values through S5 for the two *G. sacculifer* morphotypes are significantly correlated ($N = 23$; $R^2 = 0.58$), the *G. sacculifer* types with sac-like final chamber also belong in this group. Whatever additional forcing was associated with S5, it must have been small enough to have virtually no impact on some species (*Neogloboquadrina pachyderma* (d) and *Globorotalia scitula*), yet at times strong/concentrated enough to seriously influence others (most notably white *G. ruber*).

The main additional control on foraminiferal $\delta^{18}\text{O}$ at times of sapropel formation was freshwater addition, mostly associated with monsoon intensification during the precession-related insolation maxima (for overviews, see Rossignol-Strick et al., 1982; Rossignol-Strick, 1983, 1985; Jenkins and Williams, 1984; Rohling, 1994, 1999; Rohling and De Rijk, 1999; Cramp and O'Sullivan, 1999; Rohling et al., 2002; Emeis et al., 1998, 2000, 2003). Especially the trends in $\delta^{18}\text{O}$ of *Globigerinoides ruber* (w), a shallow-dwelling species in the present-day Mediterranean (Hemleben et al., 1989; Pujol and Vergnaud-Grazzini, 1995; Reiss et al., 1999), show high-amplitude variability through S5 that suggest an important impact of freshwater dilution (Figs. 2 and 5). Resistance of *G. ruber* (w) to freshwater disturbances at the very surface might also explain its shift to anomalously low $\delta^{13}\text{C}$ values within S5, as a consequence of the light terrestrial values in runoff (Figs. 2 and 5). It is one of the most euryhaline species (Hemleben et al., 1989), and so may achieve a competitive advantage in freshwater-disturbed surface ecosystems. *G. ruber* (w) has been observed in the Caribbean as the only species to inhabit freshwater-diluted lenses from the Ama-

zon/Orinoco (Schmuker, 2000; Schmuker and Schiebel, 2002).

There is a significant positive correlation ($N = 55$; $R^2 = 0.41$; $\delta^{18}\text{O}_{O. universa} = 0.58 \delta^{18}\text{O}_{G. ruber} + 0.63$) between the actual $\delta^{18}\text{O}$ values of *Globigerinoides ruber* (w) and *Orbulina universa* within S5, which suggests a similar but roughly half-amplitude response in $\delta^{18}\text{O}_{O. universa}$ relative to $\delta^{18}\text{O}_{G. ruber}$ (w) (Figs. 2 and 5). A muted impact of freshwater anomalies on $\delta^{18}\text{O}_{O. universa}$ seems supported by its weak $\delta^{13}\text{C}$ change through the sapropel (Figs. 2 and 5). As the peak monsoon flooding occurs in late summer, we 'place' both species mostly within the summer mixed layer, in agreement with their present-day peak season in the basin (Pujol and Vergnaud-Grazzini, 1995; Reiss et al., 1999). During the monsoon runoff peak, the 'normal' summer mixed-layer conditions became disturbed by freshwater-diluted layers/lenses, creating habitats that were particularly favoured by *G. ruber* (w). *O. universa* on the contrary appears to have favoured more 'normal' summer mixed-layer conditions outside the flooding season and/or below the lenses, which would agree with its preference for deeper waters in the mixed layer during part of its life cycle (e.g. Hemleben et al., 1989).

The discontinuous presence of *Globigerinoides sacculifer* morphotypes through S5 makes interpretations less straightforward, but its $\delta^{18}\text{O}$ and $\delta^{13}\text{C}$ trends (Figs. 2 and 5) essentially suggest rather similar living conditions to those of *Orbulina universa*. Note that the low $\delta^{18}\text{O}$ value for *G. sacculifer* (*trilobus* type) in the interval within S5 where *O. universa* shows heavy values is based on one possible analysis only. With no significant distinction between the isotope records of the two *G. sacculifer* morphotypes, we envisage that both are typical of the 'normal' summer mixed layer conditions, similar to *O. universa*, possibly spending (part of) the lifecycle at some depth within that layer. This would agree with observed habitats in other regions (e.g. Hemleben et al., 1989; Bijma and Hemleben, 1994).

A strengthening of the 'biological pump' should theoretically result in heavier $\delta^{13}\text{C}$ values in shallow waters (*Orbulina universa*, *Globigerinoides sacculifer*), but we observe no shift in the $\delta^{13}\text{C}$ values

of these species with the onset of S5, or even the opposite – a weak shift to lighter values (Figs. 2 and 5). In view of the considerable amounts of isotopically light terrestrial runoff (white *Globigerinoides ruber*), however, the absence of an enrichment in $\delta^{13}\text{C}$ values through S5 does not necessarily imply that there was no increase in export production. Averaged over the whole thickness of the summer mixed layer, to affect *O. universa* and *G. sacculifer*, the freshwater-related anomaly may have caused a moderate shift to lighter values that offset any enrichment due to strengthening of the biological pump. Alternatively, the monsoon flooding may have affected light penetration sufficiently to reduce the photosynthetic activity of symbionts, allowing shell formation from a carbon pool with lighter $\delta^{13}\text{C}$ values (Spero and Williams, 1988; Spero, 1992; Spero and Lea, 1993). Symbiont-bearing species more affected by the freshwater discharge (*G. ruber* (w)) would then show a stronger shift to low $\delta^{13}\text{C}$ values, while species that were less affected (*O. universa*, *G. sacculifer*) show negligible effects. In any case, it is apparent that the carbon isotopes cannot be used in a straightforward manner to assess the strength of the biological pump associated with S5; a comprehensive carbon box model would be needed.

The $\delta^{13}\text{C}$ record of *Globigerinella siphonifera* is virtually featureless. The values within S5 are weakly lighter than above and below the sapropel, but within S5 the various mean values cannot be statistically distinguished from one another (Figs. 2 and 5). The $\delta^{18}\text{O}$ values are generally heavy, with a shift to lighter values within the sapropel, similar to the records of *Neogloboquadrina pachyderma* (d) and *Globorotalia scitula*. The $\delta^{18}\text{O}_{G. siphonifera}$ record is featureless through S5, apart from slightly more depleted and more variable values in the early part relative to the rest. Variability in both the $\delta^{18}\text{O}$ and $\delta^{13}\text{C}$ records is identical when calculated for raw values over the entire S5 interval and when calculated after means-subtraction (Table 4), which highlights the absence of significant longer-term trends. The species therefore appears to have been continuously secreting its test in the same type of conditions. The water mass in which *Globigerinella siphonifera* lived does not appear to have become isolated for any significant period of time during sapropel formation, as there is only a moderate shift to lighter $\delta^{13}\text{C}$ values associated with S5, and no trend to increasingly depleted values (Figs. 2 and 5).

The low variability in both the C and O isotope records of *Globigerinella siphonifera* suggests that

Table 4

Summary of the stable isotope ranges and variability within S5 for the various species analysed, and their inferred palaeohabitat based on the qualitative arguments in Section 4.1

	N	Mean $\delta^{18}\text{O}$	Variability ^a	Mean $\delta^{13}\text{C}$	Variability ^a	Inferred habitat ^b
<i>G. ruber</i> (w)	45	−0.87	0.35 (0.57)	+0.07	0.18 (0.27)	Fresh–S.ml
<i>G. ruber</i> (p)	43	−1.32	0.33 (0.38)	+0.63	0.33 (0.37)	Spring?
<i>G. sacculifer</i>	27	−0.83	0.48 (0.49)	+1.10	0.24 (0.31)	S.ml
<i>G. sacculifer</i> (tril.)	26	−1.07	0.33 (0.50)	+1.24	0.24 (0.35)	S.ml
<i>O. universa</i>	47	+0.03	0.34 (0.41)	+1.23	0.21 (0.30)	S.ml
<i>G. glutinata</i>	30	−0.25	0.42 (0.50)	−0.71	0.43 (0.61)	Spring
<i>G. bulloides</i>	41	−0.23	0.62 (0.60)	−1.06	0.47 (0.51)	Spring
<i>H. pelagica</i>	15	−0.35	0.48 (0.62)	−0.79	0.24 (0.31)	
<i>G. siphonifera</i>	47	+0.67	0.32 (0.33)	−0.23	0.21 (0.21)	Winter ml
<i>N. pachyderma</i> (d)	17	+0.43	0.22 (0.39)	−1.41	0.31 (0.59)	Ssth/Int
<i>G. scitula</i>	18	+0.69	0.28 (0.38)	−1.50	0.19 (0.27)	(Ssth)/Int

These inferred habitats are further assessed with a box-model (Section 4.2), and the end-results are compared with modern observations in Table 5.

^a Non-bracketed values: mean of the 1 σ values for the four key intervals within S5 (in effect a detrended variance estimate). Bracketed values: straight 1 σ values through entire S5. A large offset between the two indicates underlying trends through S5.

^b Abbreviations: S.ml., summer mixed layer; Spring, spring bloom conditions; Winter ml., winter mixed layer; Ssth, summer subthermocline waters; Int., intermediate water; Fresh–Sml, freshwater affected layer/lenses in the summer mixed layer.

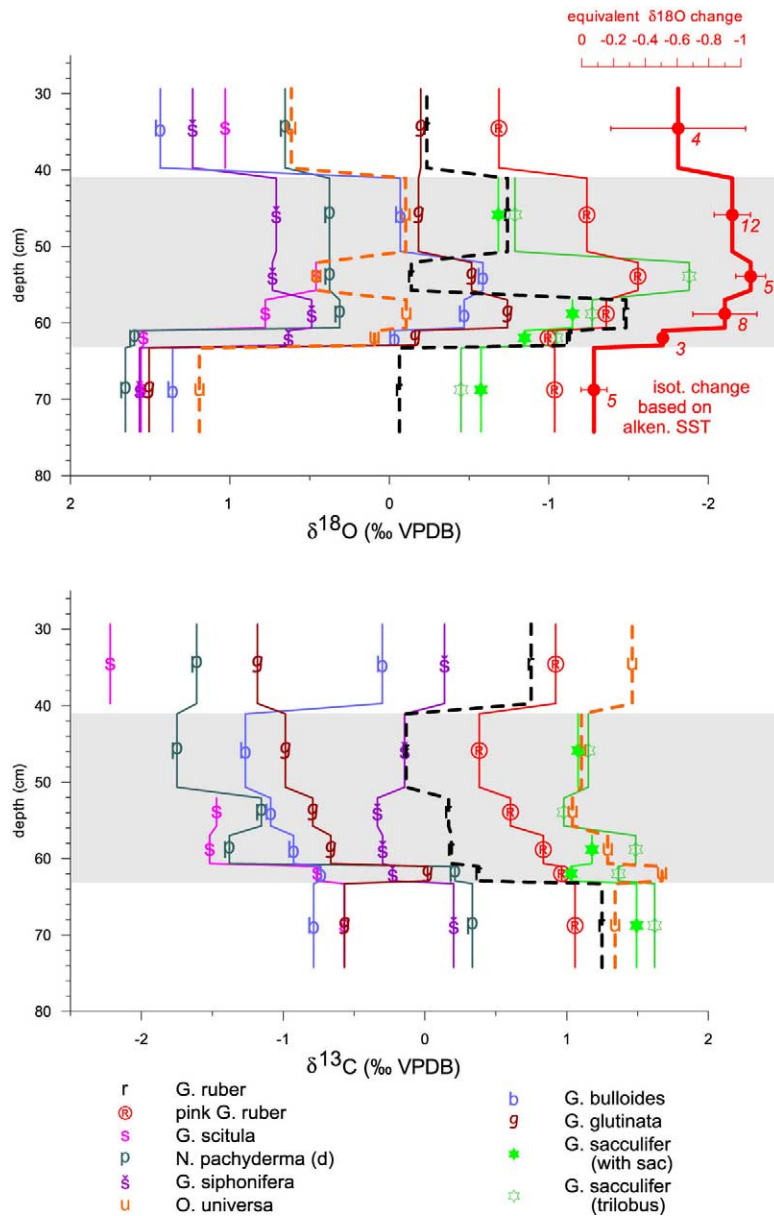


Fig. 5. Changes in the mean $\delta^{18}\text{O}$ and $\delta^{13}\text{C}$ values of the various species analysed for the intervals identified in Table 2a,b through sapropel S5 in core KS205, all plotted on the same scale. Grey band is the visible extent (dark colouration) of S5.

it inhabited a well-mixed water mass of considerable volume. This is particularly exemplified by the visible but muted expression of the freshwater-related $\delta^{18}\text{O}$ anomalies seen in *Globigerinoides ruber* (w). In fact, the $\delta^{18}\text{O}_{G. siphonifera}$ values show significant positive correlations with both $\delta^{18}\text{O}_{G. ruber}$ (w) and $\delta^{18}\text{O}_{O. universa}$ (with $N=55$,

$R^2=0.23$, $\delta^{18}\text{O}_{G. siphonifera} = 0.35 \delta^{18}\text{O}_{G. ruber} + 1.05$; and $N=57$, $R^2=0.35$, $\delta^{18}\text{O}_{G. siphonifera} = 0.47 \delta^{18}\text{O}_{O. universa} + 0.71$ respectively). These relationships crudely demonstrate that where $\delta^{18}\text{O}_{O. universa}$ responded with a similar fluctuation but of reduced amplitude to an environmental (freshwater) forcing that drove strong shifts in

$\delta^{18}\text{O}_{G. ruber (w)}$, the same is true for $\delta^{18}\text{O}_{G. siphonifera}$ but with an even further reduced amplitude. The amplitude reduction from $\delta^{18}\text{O}_{G. ruber (w)}$ to $\delta^{18}\text{O}_{O. universa}$ was related to mixing of an initially concentrated signal over the larger volume of the summer mixed layer. The further amplitude reduction to that in $\delta^{18}\text{O}_{G. siphonifera}$ then suggests a further dilution of the initial signal, which immediately hints at the impact of deep homogenisation in the winter mixed layer. Overall, it appears that *G. siphonifera* thrived in a well ventilated (not isolated) and rather eutrophic (^{12}C enriched, possibly because of turbulent nutricline erosion) water mass that may have been relatively cold, based on the species' heavy $\delta^{18}\text{O}$ signature: the winter mixed layer.

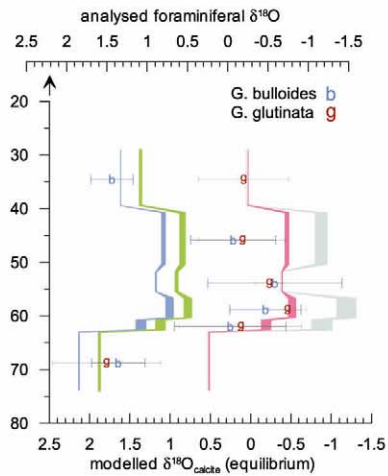
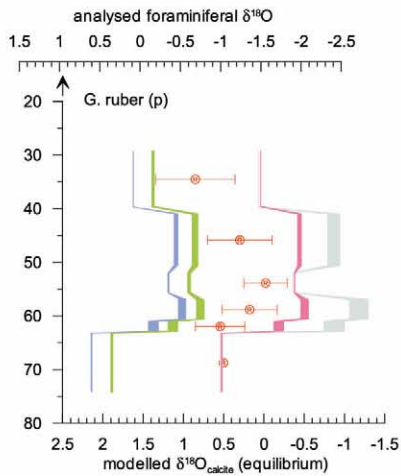
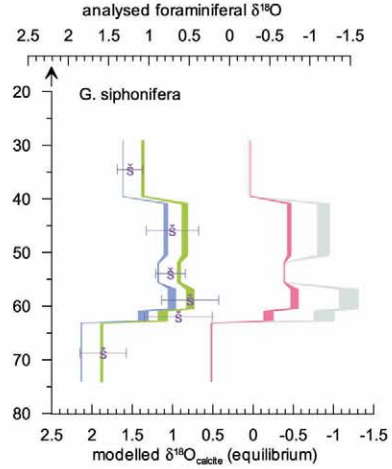
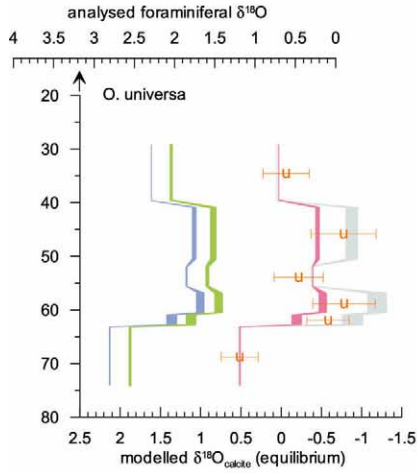
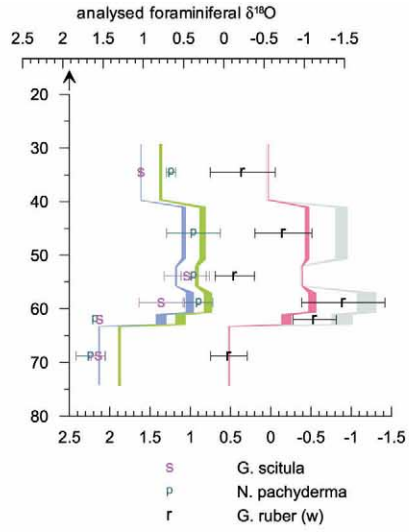
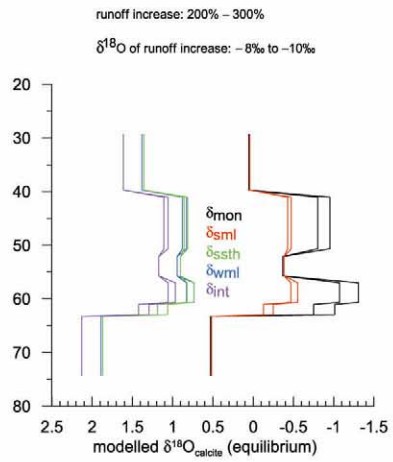
Winter-water conditions are also reflected in the $\delta^{18}\text{O}$ records of *Globorotalia scitula* and *Neoglobobuadrina pachyderma* (d), with low-amplitude variability around very heavy mean values (Figs. 2 and 5). Their $\delta^{13}\text{C}$ values, however, place these species in a totally different environment than *Globigerinella siphonifera* (Figs. 2 and 5; Table 4). Both *G. scitula* and *N. pachyderma* (d) show shifts to extremely light $\delta^{13}\text{C}$ values, with trends of increasing depletion, through sapropel S5. The combined data suggest habitats within a winter-type water mass that was isolated for extended periods of time, allowing long-term build-up of ^{12}C -rich remineralisation products. We infer, therefore, that these two species lived at considerable depth in winter-type waters, near/in the nutricline. This places them possibly in a summer subthermocline setting, but more likely in close association with the more persistently isolated intermediate waters. As argued above, the great 'stability' in the $\delta^{18}\text{O}_{G. scitula}$ and $\delta^{18}\text{O}_{N. pachyderma (d)}$ implies that their signals have been processed through a 'giant capacitor', which systematically removed all high-frequency variability to leave only the main trends. This supports a main habitat in the intermediate water.

Finally, there are three species that lack any systematic behaviour in their oxygen and carbon isotope records: *Globigerinoides ruber* (pink), *Globigerina bulloides*, and *Globigerinita glutinata*. *G. ruber* (pink) consistently shows the lightest $\delta^{18}\text{O}$ values of all species investigated (Fig. 5), which

would suggest the warmest/freshest habitat. However, it shows relatively small amplitudes of change between the various mean values (Figs. 2 and 5). This is not what would be expected anywhere in the summer mixed-layer (e.g. *Orbulina universa*, *Globigerinoides sacculifer*), or indeed in the very surface levels with impact of monsoon runoff (*G. ruber* (w)). Instead, the pattern of shifts between the mean $\delta^{18}\text{O}$ and $\delta^{13}\text{C}$ values for *G. ruber* (p) is very similar to that for *G. bulloides*, except that it seems to be offset by -1 to -1.5‰ ($\delta^{18}\text{O}$) and $+1.5$ to $+2\text{‰}$ ($\delta^{13}\text{C}$) relative to *G. bulloides*. The short-term variability, in contrast, is much lower in *G. ruber* (p) than in *G. bulloides* (Figs. 2 and 5; Table 4). Evidently, they are not simply systematically offset from one another, which precludes a conclusion that both lived under similar conditions but with different deviations from equilibrium. *G. glutinata* shows very similar signals to those of *G. bulloides* (Figs. 2 and 5; Table 4).

As discussed before, a lack of systematic signal such as observed in *Globigerina bulloides*, *Globigerinita glutinata*, and *Globigerinoides ruber* (p), should be expected for species that prefer seasonal 'transitions', e.g. the autumn breakdown of stratification, or the build-up of stratification in spring. This is a proxy relationship, since *G. bulloides* and *G. glutinata* in reality depend less on radiation than on deep nutrient entrainment by storms (both spring and fall; Schiebel et al., 2001). The insensitivity of these species' $\delta^{18}\text{O}$ records to the freshwater-related anomalies witnessed by *G. ruber* (w) (Figs. 2 and 5) then suggests that they are not from the autumn, which follows shortly after the peak monsoon flooding, but instead were associated predominantly with the spring 'bloom'. Possibly, their erratic $\delta^{18}\text{O}$ signatures reflect variable depth habitats and the early development of (thermal) differentiation within the mixed layer. The observed differences in short-term variability between $\delta^{18}\text{O}_{G. bulloides}$, $\delta^{18}\text{O}_{G. glutinata}$, and $\delta^{18}\text{O}_{G. ruber (p)}$ then suggest growth conditions over more extensive depth ranges for *G. bulloides* and *G. glutinata*, and a more narrowly constrained range (towards the surface?) for *G. ruber* (p).

An inferred spring-bloom habitat for *Globige-*



rina bulloides and *Globigerinita glutinata* would be consistent with modern observations of cosmopolitan and eutrophic/opportunistic preferences (cf. Hemleben et al., 1989; Pujol and Vergnaud-Grazzini, 1995; Reiss et al., 1999; Schiebel and Hemleben, 2000). However, it is a controversial suggestion for *Globigerinoides ruber* (p). It would imply that *G. ruber* (pink) secretes its shell in great disequilibrium, which may not be supported by observations (Deuser and Ross, 1989; Table 2a,b). It appears that we cannot deduce a realistic palaeohabitat for this species on the basis of the available data.

4.2. Model-based habitat assessment

Fig. 6 shows the modelled equilibrium calcite $\delta^{18}\text{O}$ values for the various boxes. Two lines are displayed for each box. The lighter values represent the solution using a monsoon runoff $\delta^{18}\text{O}$ composition of -10‰ , and the heavier values represent a scenario that uses -8‰ . The lower ‘lobe’ of S5 was set to have a monsoon intensification factor $M=3$, and the upper ‘lobe’ was set with $M=2$ (Table 3). A complete collapse of the monsoon intensification was prescribed for the interval with heavy $\delta^{18}\text{O}_{G. ruber(w)}$ and $\delta^{18}\text{O}_{O. universa}$ values (Figs. 1, 2 and 5). The specified range of monsoon intensity values is chosen: (a) to offer a range of simulations that portrays the model’s sensitivity to strong extremes in M ; and (b) so that the general underlying trends in the simulations are in basic agreement with the records. Sensitivity tests are discussed in Section 4.5.

The dominant impact of a monsoon flood of isotopically light freshwater is observed in the small-volume monsoon box. Note, however, that this box also sustains all evaporation during its two-month life span (a high flux at the high T_s values). This considerably counteracts the salinity

and $\delta^{18}\text{O}$ impacts of the flood. Mixed over the more voluminous summer mixed-layer box, the isotopic anomaly becomes strongly muted. The winter mixed-layer and summer subthermocline boxes, as expected, show virtually identical $\delta^{18}\text{O}_{\text{calcite}}$ values, and there is a systematic (1°C -equivalent) enrichment in the intermediate-water values relative to the winter boxes.

We next compare the modelled traces with the various species’ mean values in the six key intervals. The model approaches the same intervals, since it relies on the seasonal temperature values derived from the mean alkenone-SST values for the same intervals (Fig. 6). The analytical series are shifted until, in order of priority, best visual fits are obtained: (1) in the pre-sapropel interval; and (2) over the entire trace. This procedure offers a first-order insight into the (dis-)equilibrium state of the foraminiferal calcite, which is more extensively discussed in Section 4.3. Fig. 7 compares the actual data with the modelled traces, using the offsets determined in Fig. 6.

The data for *Globigerinoides ruber* (w), *Globorotalia scitula*, and *Neogloboquadrina pachyderma* (d) agree well with the modelled traces, with the simulated contrast between winter and summer/monsoon-box conditions close to that observed between the *N. pachyderma* (d)–*G. scitula* pair and *G. ruber* (w). The modelled long-term variability also agrees well with that in the observations for the winter-water species, but for *G. ruber* (w) the amplitude is underestimated. We were not able to drive the model simulations to the very heavy values indicated by $\delta^{18}\text{O}_{G. ruber(w)}$ in the ‘interruption’ without disturbing the close agreement in the other boxes with the analytical series of *N. pachyderma* (d), *G. scitula*, *Orbulina universa*, and *Globigerinella siphonifera* (Figs. 6 and 7). Moreover, comparison of the modelled traces with $\delta^{18}\text{O}_{G. ruber(w)}$ variability through S5 in ODP sites 971A and 967C suggests that the main run

Fig. 6. Comparison between the modelled traces of $\delta^{18}\text{O}$ for equilibrium calcite (see text) and the mean values of $\delta^{18}\text{O}$ of the various species in the key intervals through S5 in core KS205 (Table 2a,b; Fig. 2). All values in ‰ VPDB. The analytical series are simply shifted to obtain the best agreement in trends and absolute values (see text), and the inferred offsets are evaluated in comparison with observed offsets of the various species from isotopic equilibrium (Section 4.3). Abbreviations: mon, monsoon box; sml, summer mixed layer; ssth, summer sub-thermocline layer; wml, winter mixed layer; int, intermediate water.

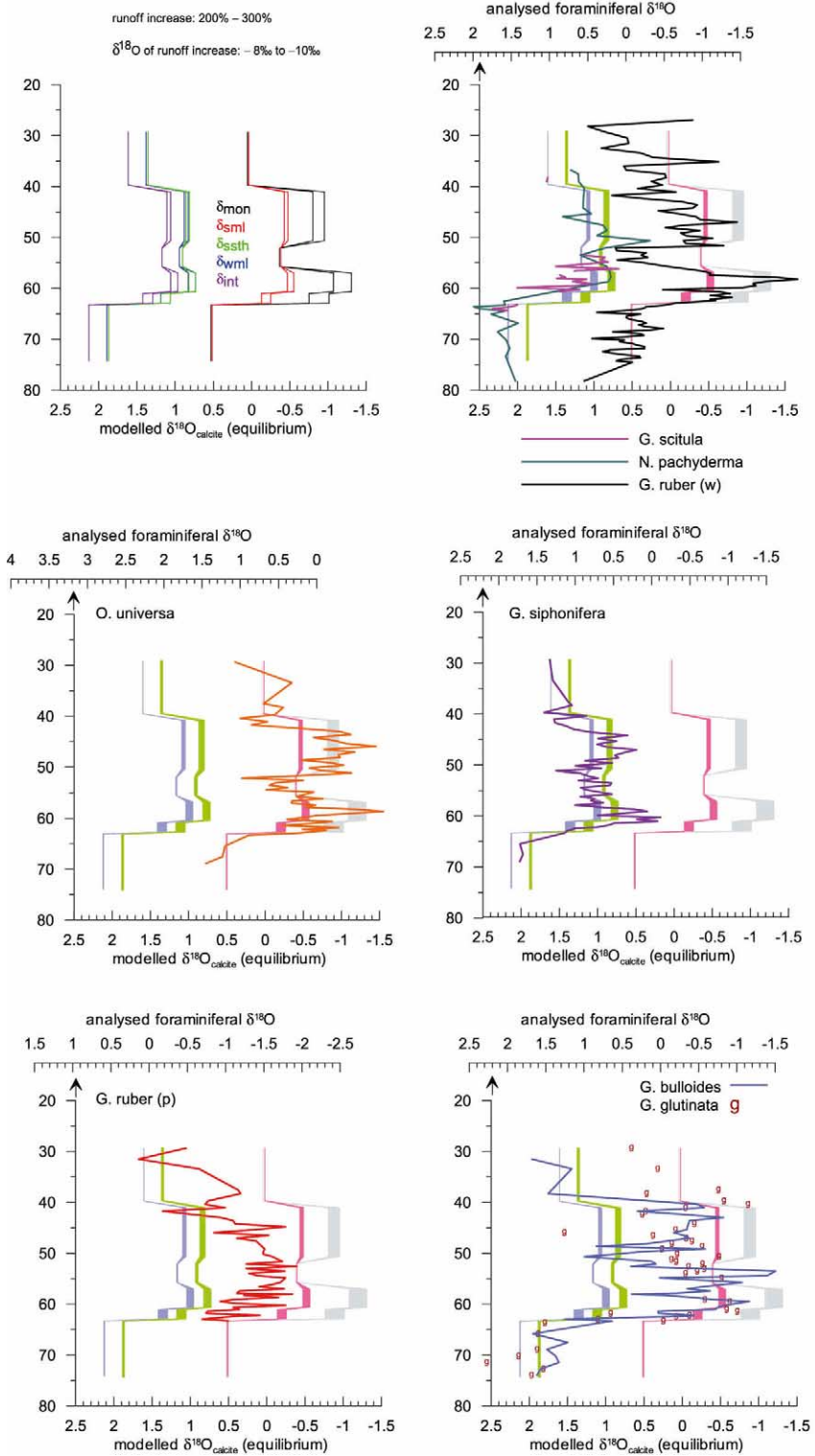


Fig. 7. As Fig. 6, but for the actual data rather than means+standard deviations. The inferred offsets between analytical scales and equilibrium scales are kept exactly identical in Figs. 6 and 7.

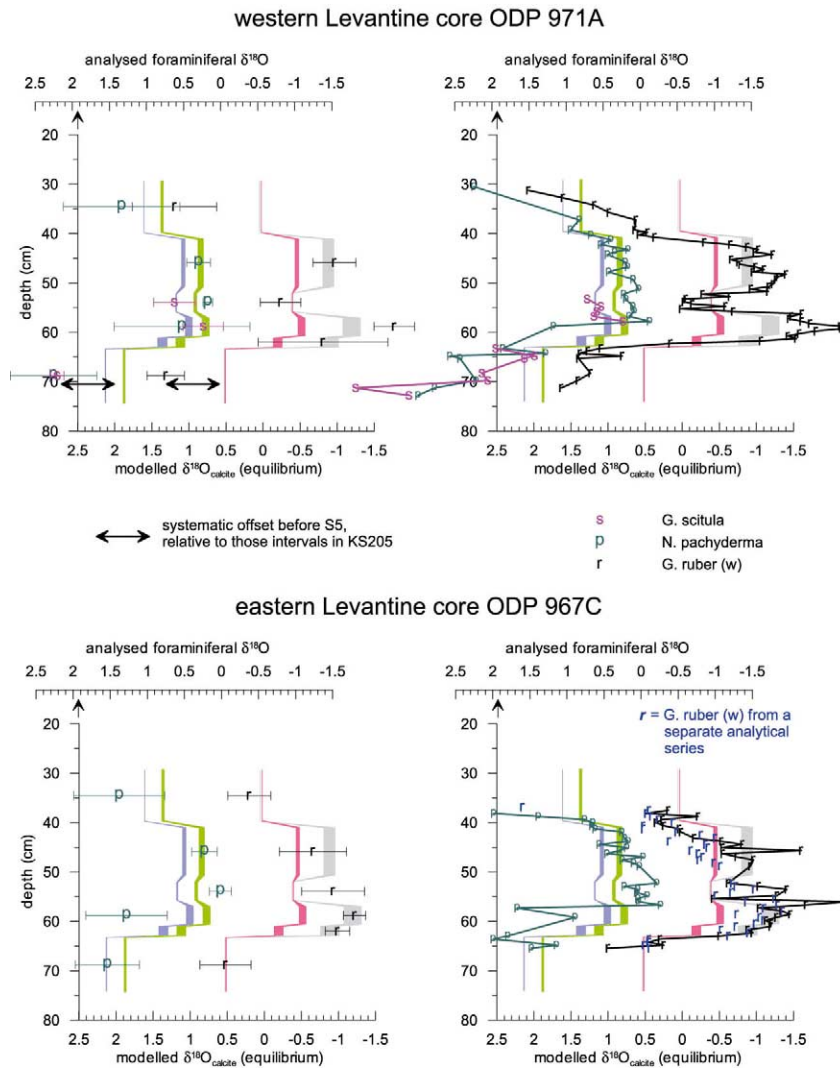


Fig. 8. As Figs. 6 and 7, but now for the data in S5 of ODP Holes 971A and 967C. The inferred offsets between analytical scales and equilibrium scales are again kept exactly identical to those in Figs. 6 and 7.

yields a satisfactory trace for this species (971A), or even overestimates the enrichment (967C) (Fig. 8). We infer that the model reasonably approximates the actual changes in $\delta^{18}\text{O}_{G. ruber (w)}$ on a basin-wide scale, and that other (not included) influences caused regional deviations.

Orbulina universa shows considerable longer-term variability, and it would appear to fit best ‘in between’ the modelled summer mixed-layer and monsoon box conditions (Figs. 6 and 7). This would imply that *O. universa* occupied the

more ‘normal’ summer mixed-layer conditions in between and/or below, but for part of its life cycle affected by, freshwater-dilution at the very surface.

Globigerinella siphonifera shows a virtually in-equilibrium match with the modelled $\delta^{18}\text{O}_{\text{calcite}}$ record for winter-type waters (Figs. 6 and 7). The good results from the model for this species, as well as *Neogloboquadrina pachyderma* (d), *Globorotalia scitula*, and also *Orbulina universa*, inspire considerable confidence in the model’s basic

underlying assumptions such as the rough estimates for the monsoon-box thickness and the monsoon intensification factor. Note, for example, that an increase in the thickness of the monsoon box would necessitate an increase in the monsoon floods to obtain the same isotopic anomalies in *Globigerinoides ruber* (w) (and *Orbulina universa*). However, that signal then becomes too dominant in the winter-water boxes, upsetting the good correspondence observed in the main run for *G. siphonifera*, *O. universa*, *N. pachyderma* (d) and *G. scitula* in KS205 as well as sites 971A and 967C.

The data for *Globigerinoides ruber* (p), *Globigerina bulloides*, and *Globigerinita glutinata* remain difficult to place (cf. Section 4.1). We proposed that *G. ruber* (p), *G. bulloides* and *G. glutinata* thrived in spring, reflecting the transition from winter-type conditions to summer-type conditions. Their isotopic (dis-)equilibrium states may then be tentatively estimated by shifting the records so that the bulk of values falls between the winter and summer ‘extremes’ (Figs. 6 and 7).

4.3. Assessment of the model-inferred offsets from equilibrium $\delta^{18}\text{O}$

The model does not allow for such processes as entrainment and mixing between the separate boxes, and also has simply prescribed, basin-averaged seasonal temperature and air humidity conditions. Comparisons between the simulated and analysed $\delta^{18}\text{O}$ values (Figs. 6–8) are therefore most reliable where relative trends and offsets are concerned. Although the simulated absolute $\delta^{18}\text{O}_{\text{calcite}}$ values deserve more caution, the inferred isotopic disequilibria for the various species still provide a useful criterion for gauging the general quality of the model-based reconstructions. Note that 1σ ranges around the analysed means used to evaluate the disequilibria amount to ± 0.2 – 0.6‰ (Table 4), and that additional bias may occur due to deviations of the species’ actual growth temperatures from the applied schematic seasonal temperature variations.

For *Globigerinoides ruber* (w), *Neogloboquadrina pachyderma* (d), and *Globorotalia scitula*, the best fit to modelled $\delta^{18}\text{O}_{\text{calcite}}$ invokes an offset

of roughly -0.6‰ , which is within the 1σ range from values observed in culture experiments with *G. ruber* (w) and *N. pachyderma* at $\sim 20^\circ\text{C}$ or in plankton tow samples of *G. scitula* (Table 2a,b). For *Globigerina bulloides*, the tentatively inferred offset is roughly -0.3‰ , which would be around 1‰ heavier than suggested by culture experiments at 20°C (Table 2a,b). The model-suggested offset of -0.3‰ for *Globigerinella siphonifera* is in reasonable agreement with warm-water plankton tow results of -0.55‰ (Table 2a,b). Culture experiments suggest that *Orbulina universa* secretes its test at -1.0 to -0.7‰ relative from equilibrium at $\sim 20^\circ\text{C}$ (Table 2a,b). The difference between these values and our inferred offset of $+0.7\text{‰}$ is rather large, but we note that Spero and Williams (1988) reported very different $\delta^{18}\text{O}_{O. universa}$ values near equilibrium (± 0.2 – 0.4‰), which would be within our 1σ limits. The inferred offsets from equilibrium for *G. ruber* (p) is around -1.5‰ , which exceeds some observations (Deuser and Ross, 1989) but may find some support from warm-water plankton tow results that show an offset of 0.0 to -0.4‰ relative to *G. ruber* (w) (Table 2a,b), giving *G. ruber* (p) a total offset between -0.6 and -1.0‰ that approaches the 1σ limit (Table 4) around our model-estimated value of -1.5‰ .

4.4. Model-based insight into the salinity: $\delta^{18}\text{O}$ relationship

The model simultaneously resolves for salinity, $\delta^{18}\text{O}_{\text{water}}$, and $\delta^{18}\text{O}_{\text{calcite}}$. It therefore determines the seawater $S:\delta^{18}\text{O}_{\text{water}}$ relationship for the various boxes. With the monsoon intensification factor (M) set to values of 3 and 2 for the lower and upper lobes of S5, respectively (Table 3), two sets of solutions were obtained: one using a $\delta^{18}\text{O}$ of monsoon runoff of -8‰ , and the other using -10‰ (Fig. 9). For salinity, both solutions are identical, but the simulated $\delta^{18}\text{O}$ records differ considerably. The right-hand panels of Fig. 9 illustrate the $S:\delta^{18}\text{O}_{\text{water}}$ relationships in the various boxes. The use of a different isotopic ratio for the monsoon runoff considerably alters the temporal $S:\delta^{18}\text{O}_{\text{water}}$ slopes. There also is a considerable difference between the temporal $S:\delta^{18}\text{O}_{\text{water}}$

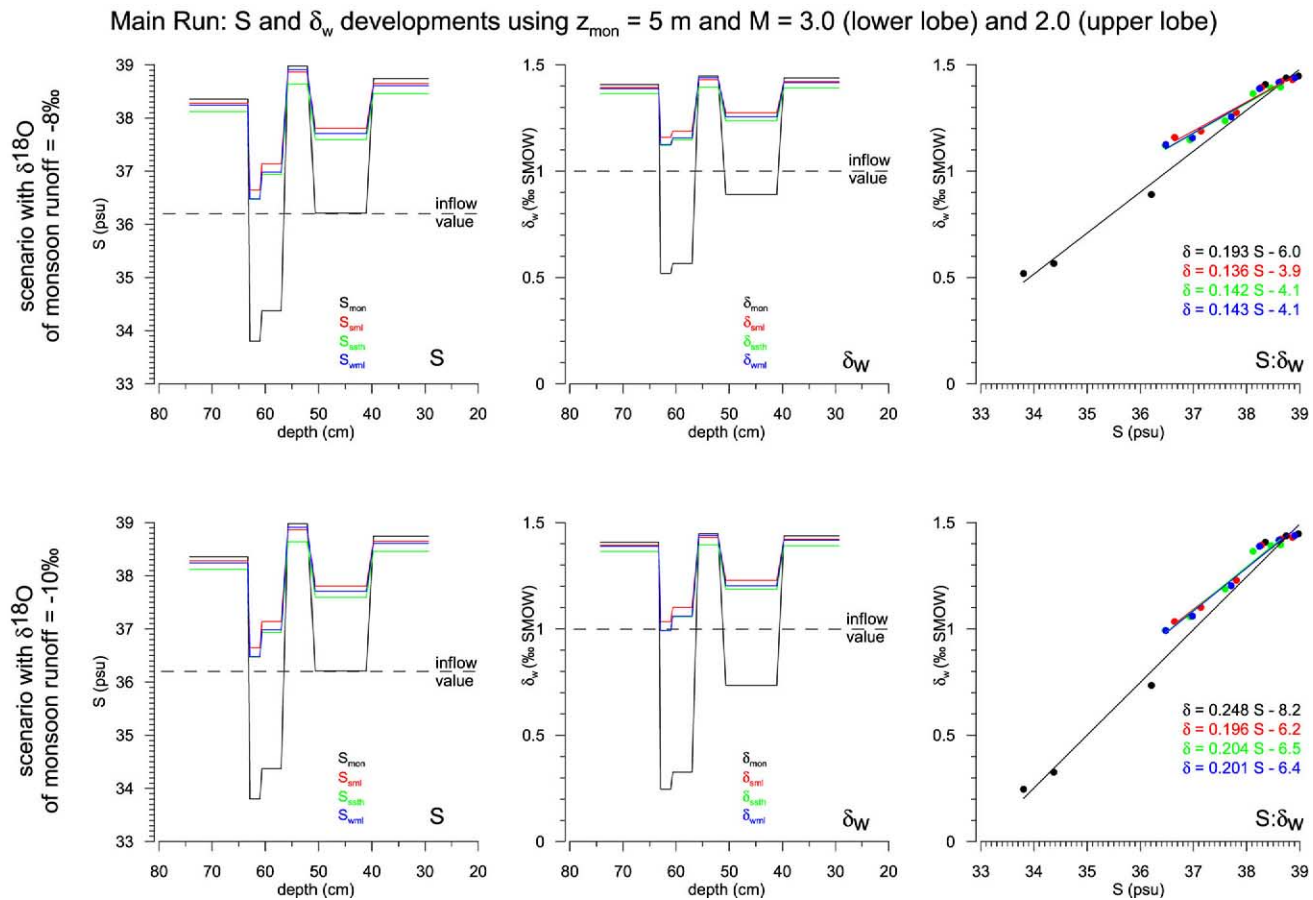


Fig. 9. Assessment of the $S:\delta^{18}\text{O}_{\text{water}}$ relationships in the main model run using $z_{\text{mon}} = 5$ m and $M = 3.0$ (lower lobe) and 2.0 (upper lobe). The impacts of two scenarios are evaluated: (1) monsoon runoff $\delta^{18}\text{O} = -8\text{‰}$ (top panels); and (2) monsoon runoff $\delta^{18}\text{O} = -10\text{‰}$ (see text Section 4.4).

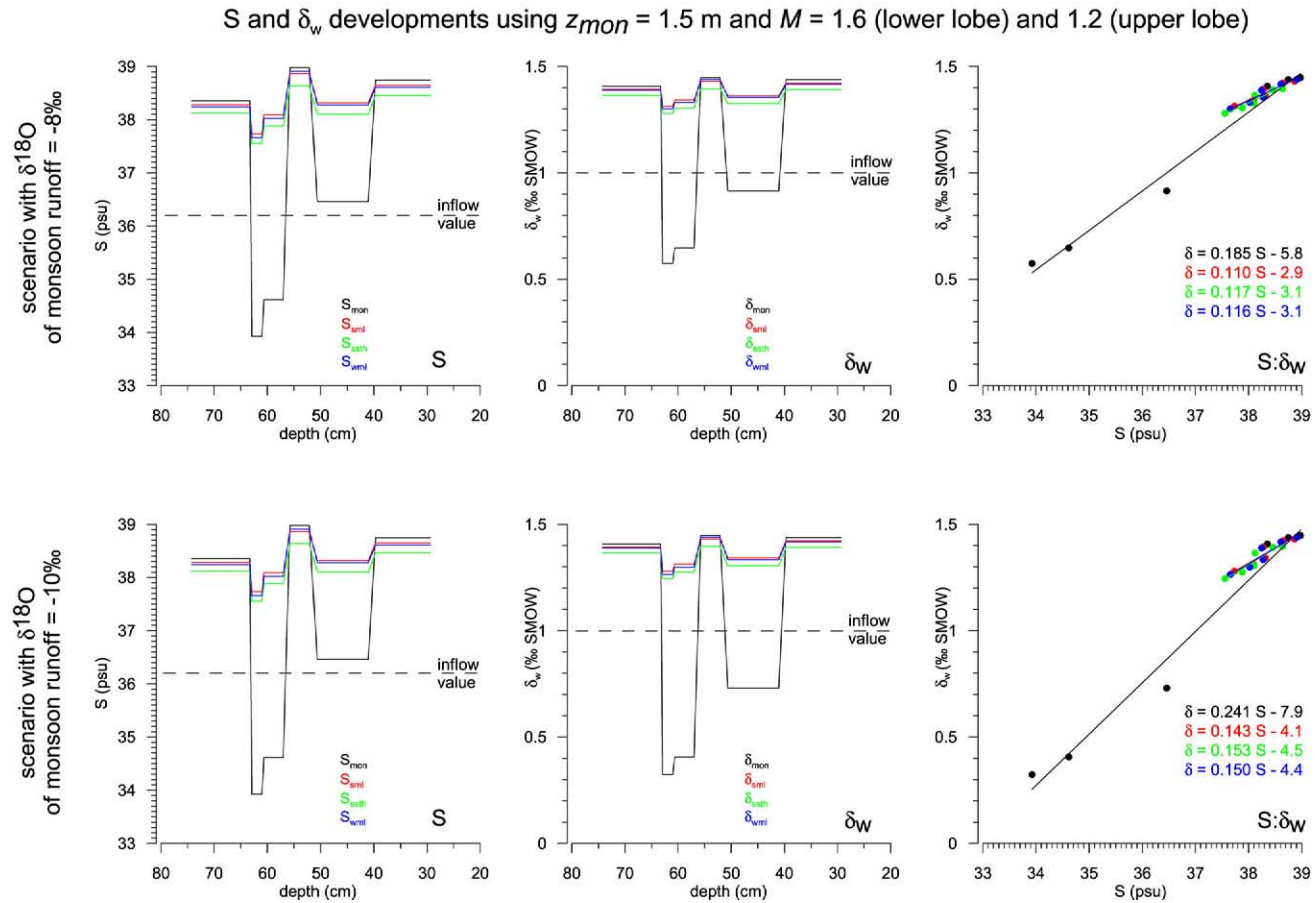


Fig. 10. As Fig. 9, but here to investigate sensitivity to a change in model set-up, to $z_{mon} = 1.5$ m, for $M = 1.6$ (lower lobe) and 1.2 (upper lobe) (see text Section 4.5 for explanations).

slope of the monsoon box and the other boxes, within any single simulation experiment. If this were overlooked, then reconstructions based on $\delta^{18}\text{O}_{G. ruber(w)}$ would strongly overestimate the amount of change in the basin's hydrological forcing. It is further evident that $\delta^{18}\text{O}_{G. bulloides}$, $\delta^{18}\text{O}_{G. ruber(p)}$ and $\delta^{18}\text{O}_{G. glutinata}$ are also unsuitable for reconstructions of the basin's overall circulation state – in these cases because of a lack of firm affinity with any of the end-member water masses.

The most useful $\delta^{18}\text{O}$ records for establishing the overall circulation state are those for *Globigerinella siphonifera*, *Neogloboquadrina pachyderma*, and *Globorotalia scitula*, since the winter-water conditions represent the most homogenised, least variable, long-term integrated response to the entire suite of possible environmental perturbations. However, even when using such representative records, and even if season/species-specific SST control were established, the fundamental problem remains that spatial and temporal $S:\delta^{18}\text{O}_{\text{water}}$ relationships are not normally the same (see also Rohling and Bigg, 1998; Rohling and De Rijk, 1999; Rohling, 1999, 2000; Schmidt, 1999a,b). We expect more profound advances from palaeo-circulation models of increasing complexity with embedded $\delta^{18}\text{O}$ calculations, validated against whole-faunal isotope data.

4.5. Sensitivity tests and monsoon intensification estimates

General sensitivity tests with the presented type of model have been reported previously (Rohling, 1999). The essential modification to be evaluated here involves the somewhat arbitrarily chosen thickness of the monsoon box. In the main run, its thickness is set at 5 m over the entire surface area of the basin. This may be an overestimate, since even at $M=3$, the equivalent of just under 1 m of total runoff is specified into the basin. The lower limit for the monsoon-box thickness can be estimated at ~ 1.5 m. Mixture of that much marine water at a salinity of ~ 38 p.s.u. with 1 m of freshwater yields an endproduct with a salinity of ~ 22 p.s.u., the absolute minimum for survival of planktic foraminifera (Hemleben et al., 1989). For a reduction in the monsoon-box volume, less

monsoon intensification would be needed to achieve roughly the same low $\delta^{18}\text{O}$ (and salinity) values in that box as found in the main run. To maintain the main run's values for the lower lobe of S5, the required monsoon intensification factor is related to the change (∂z_{mon}) in the thickness of the monsoon box as $M \approx M_0 (1 + 0.12 \partial z_{\text{mon}})$, where M_0 is the value used in the main run (Table 3). For a 1.5-m-thick monsoon box, this gives $M = \sim 1.6$ (lower lobe) and $M = \sim 1.2$ (upper lobe). Although this would not alter the temporal $S:\delta^{18}\text{O}$ ratio in the monsoon box (z_{mon} and M were changed proportionally), great shifts would result in the ratios for the other boxes (compare Figs. 9 and 10).

By defining a relatively thick (5 m) monsoon box in the main run, the model minimises the contrasts between the various boxes, in good agreement with the total range of foraminiferal $\delta^{18}\text{O}$ values. The total spread of the data spans 2.2‰ between the heaviest and lightest (consistent) mean values within S5 (Fig. 5), which is closely captured by the difference between extremes in the main run of the model (Figs. 6 and 7). Also, *Globigerinella siphonifera* shows some long-term fluctuations (Fig. 7) that agree better with the simulated patterns from the main run than with those from the experiment with a monsoon box of 1.5 m (Fig. 11). Although these are hints that the main run may be more realistic, the differences between the two experiments (Fig. 11) are mostly smaller than the short-term variability in the data. Therefore, the full range of monsoon intensifications suggested by the two experiments should be considered: during the formation of the lower (upper) lobe of S5, monsoon flooding introduced an extra 160–300% (120–200%) of runoff into the basin, compared to the present. Although these are wide ranges, they offer the first quantitative indication of the order of magnitude of the freshwater disturbances when S5 developed.

4.6. Comparison of habitats during S5 and those during Holocene S1 and the Present

Here, we compare our stable isotope records through S5 with similar data through Holocene

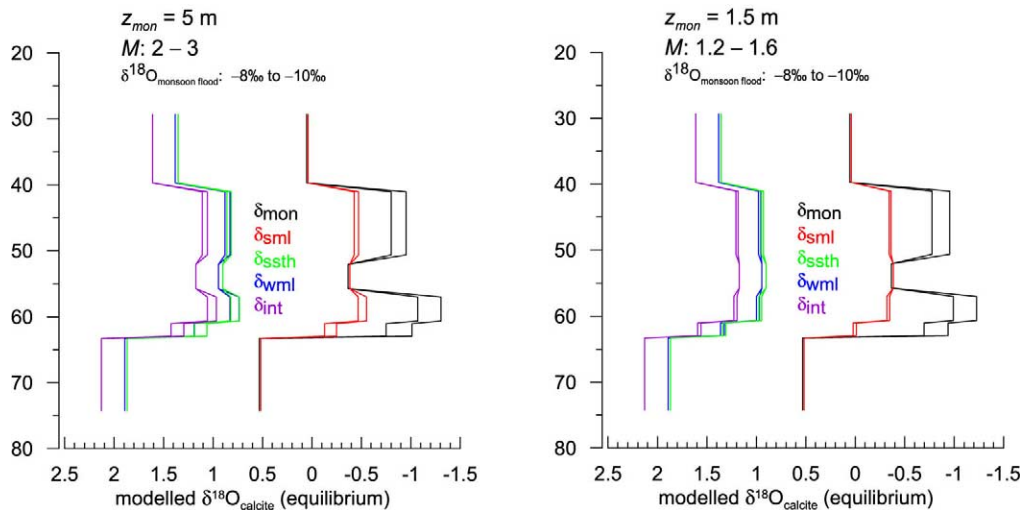


Fig. 11. Comparison between the modelled $\delta^{18}\text{O}$ traces through S5 for equilibrium calcite in the various surface and intermediate water boxes for main model run (left-hand panel; related to Fig. 9) and the sensitivity test (right-hand panel; related to Fig. 10). Abbreviations as in Fig. 6.

sapropel S1 in SE Aegean core LC21 (Fig. 12). The faunal and geochemical signals in LC21 are representative of developments in the wider Aegean Sea, and also resemble those observed in the Adriatic Sea and northern Levantine Basin (e.g. De Rijk et al., 1999; Mercone et al., 2000, 2001; Casford et al., 2001, 2002). The Holocene record adds an evaluation of *Globorotalia inflata* within the full-faunal context. This species was extremely rare through S5 (see also Corselli et al., 2002). Fig. 12 shows a Late Glacial to Holocene $\delta^{18}\text{O}$ profile for *G. inflata* that overlaps with $\delta^{18}\text{O}_{N. pachyderma}$ (d), whereas $\delta^{13}\text{C}_{G. inflata}$ resembles $\delta^{13}\text{C}_{G. ruber}$ (w). The trends and position of the *G. inflata* records relative to those of the other major species show a strong similarity to those of *Globigerinella siphonifera* through S5 (Fig. 12). We infer that *G. inflata* also inhabited the well-ventilated, deeply homogenised winter mixed layer.

The comparison between S5 and S1 (Fig. 12) further shows that the strong depletions in S5, ascribed to freshwater dilution, are much less evident in S1. As a result, there is a much smaller difference between $\delta^{18}\text{O}_{G. ruber}$ (w) and $\delta^{18}\text{O}_{G. inflata}$ in S1 than between $\delta^{18}\text{O}_{G. ruber}$ (w) and $\delta^{18}\text{O}_{G. siphonifera}$ in S5. Moreover, the apparent

summer species *Globigerinoides ruber* (w), *Orbulina universa*, and *Globigerinoides sacculifer* (*trilobus* type) show much reduced spread between one another in S1 of core LC21. This suggests that the impact of discrete freshwater-diluted lenses in the summer mixed layer was virtually negligible during the deposition of S1 in the SE Aegean Sea.

Changes in the carbon isotope records are highly comparable between S5 and S1, except where *Neogloboquadrina pachyderma* (d) is concerned. $\delta^{13}\text{C}_{N. pachyderma}$ (d) reaches very low values through S5, but there is no such strong trend in S1 of core LC21. In the central Aegean Sea, stronger shifts were found through S1 for this species, reaching -1.5‰ (Casford et al., 2002, 2003). In Aegean core LC21, some low-oxygen tolerant benthic foraminifera (*Chilostomella mediterraneensis*) survived through S1, and their values are indicated as well (Fig. 12). Their presence suggests intermittent availability of low concentrations of oxygen in bottom waters, and a more intensive phase of ventilation is thought to be responsible for the division of S1 into two discrete units (cf. De Rijk et al., 1999; Myers and Rohling, 2000; Mercone et al., 2001). It is apparent that the very negative $\delta^{13}\text{C}$ values found in the planktic species *N. pachyderma* (d) and *Gloro-*

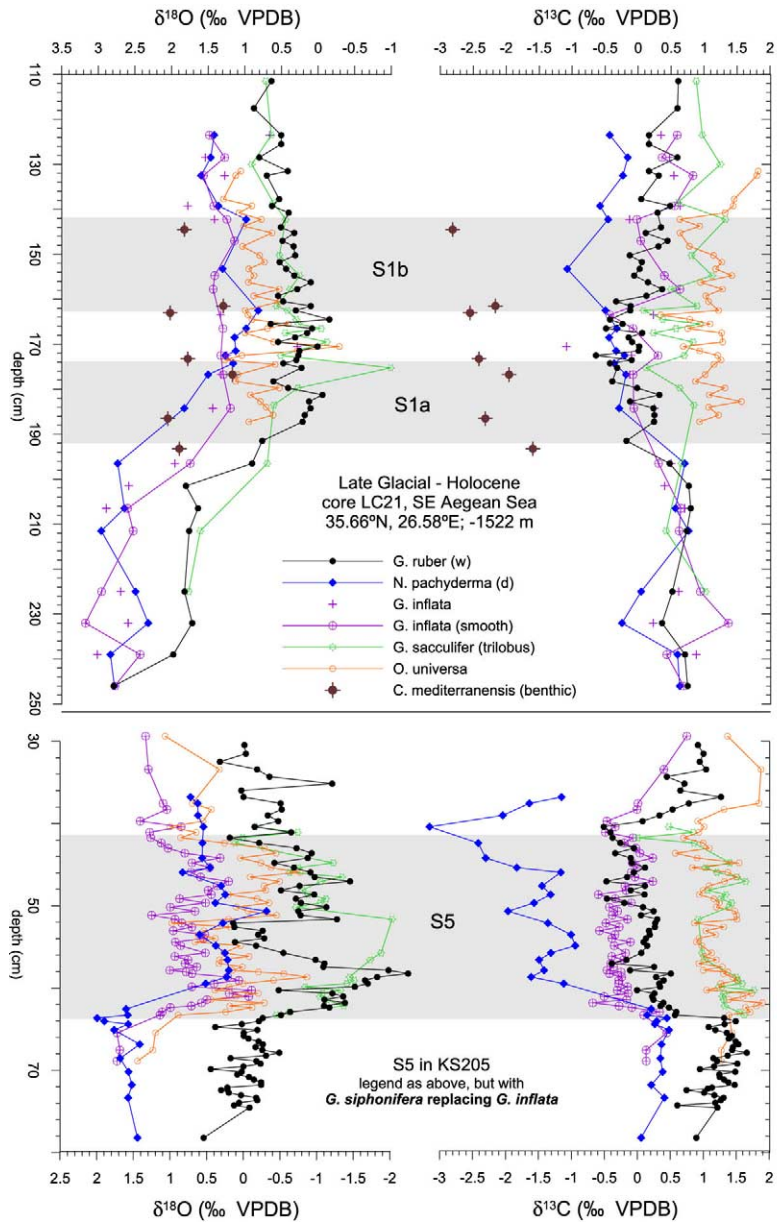


Fig. 12. Comparison between analytical $\delta^{18}\text{O}$ and $\delta^{13}\text{C}$ series for various foraminiferal species (in ‰ VPDB) through Holocene sapropel S1 in core LC21 from the SE Aegean Sea, and Eemian sapropel S5 from core KS205.

talia scitula in S5 approximate the S1 values for the benthic species *Chilostomella mediterraneis*, which lived at ~ 1500 m depth. Overall, the isotope gradients in S5 and S1 show comparable general developments, but the gradients are much stronger in S5 than in S1, while the fresh-

water dilution also appears much stronger in S5 than in S1. We infer that both sapropels reflect a similar hydrographic configuration, but that S5 represents a more 'intense' version of this configuration. The greater 'intensity' would agree with the fact that S5 commonly contains 4–10 wt% of

organic carbon, vs. 1–3 wt% for S1 (e.g. Murat, 1984; Fontugne and Calvert, 1992).

The inferred habitat characteristics for the various species during the deposition of S5, including the additional information for *Globorotalia inflata* from S1, can now be compared with the extensive (plankton tow) study of present-day foraminiferal distribution patterns in the Mediterranean presented by Pujol and Vergnaud-Grazzini (1995), and their distribution in core tops as synthesised by Thunell (1978). Both studies show that *Globigerinoides ruber* is the most ubiquitous species in the eastern Mediterranean. Although present in detectable numbers also in winter, it dominates in summer, and occupies especially the upper 50 m of the water column. Both in the living assemblages and in surface sediments, *G. ruber* is particularly dominant (> 60%) in extreme eastern locations. The diagrams for summer presented by Pujol and Vergnaud-Grazzini (1995) suggest a west–east increase in the dominance of pink types within *G. ruber*, but they emphasise that to the east of 18°E, total faunal abundances are extremely low, with domination by *G. ruber* (w). Pujol and Vergnaud-Grazzini (1995) find strong abundance maxima of spinose predatory species (notably *G. ruber* (p)) at the seasonal thermocline. In the eastern Mediterranean, *Globigerinoides sacculifer* (*trilobus*) and *Orbulina universa* prevail only in summer, and these species actually control the standing stocks in the summer mixed layer in the western basin (Pujol and Vergnaud-Grazzini, 1995). The non-spinose species *Globorotalia inflata* and *G. truncatulinoides* (not found in the present study) were found to prevail to great depth in the western basin during winter, and are also among the more important species in winter in the eastern basin. Where present, notably in the Levantine basin, *Globigerinella siphonifera* displays peak abundances in winter. The studies of Pujol and Vergnaud-Grazzini (1995) and Rohling et al. (1995) furthermore illustrate that density fronts or density gradients within the photic layer can support year-round persistence of grazing species such as *G. inflata*, *G. truncatulinoides*, *Neogloboquadrina pachyderma* (d).

It is tempting to ascribe the strong dominance of *Globigerinoides ruber* in the easternmost sector

of the basin to the impact of (pre-Aswan) Nile outflow, which under peak flood conditions caused salinities in the plume to drop to values as low as 28 p.s.u. (Reiss et al., 1999). In core GA-112 from the slope in the Ashdod area (S Israel; 31°56.41'N, 34°22.13'E; 472 m), Reiss et al. (1999) report a major abundance minimum of *G. ruber* between ~1700 (dated) and ~1000 (estimated) conventional radiocarbon years BP, which appears to form the abrupt culmination of a very gradual reduction since ~2600 years BP. Its timing is remarkably coincident with an episode of low Nile flood conditions (Hassan, 1997). However convenient these observations might seem in relation to the affinity of *G. ruber* (w) for freshwater-diluted conditions inferred here and in Rohling et al. (2002), they are suggestive only. We feel supported, however, by recent Caribbean plankton tow results from freshwater-diluted lenses that originate from the Amazon/Orinoco, which show sustained populations dominated by *G. ruber* (w) (Schmuker, 2000; Schmuker and Schiebel, 2002).

Modern observations do not link *Globigerinoides ruber* (p) with spring, as suggested in the present study. However, the unfortunate absence of a sampling in the spring season may be complicating the correct identification of the most important abundance season for many species. Alternative interpretations of *G. ruber* (p) may be possible in view of the data presented by Pujol and Vergnaud-Grazzini (1995). Possibly, the $\delta^{18}\text{O}$ record of this species is noisy because it reflects a range of temperature values resulting from its apparent living positions in both the very warm shallowest levels (upper 20 m) and in association with the considerably cooler summer thermocline. Some stations (especially 15B, south of Cyprus) even show an apparent bimodal depth distribution of *G. ruber* (p) between these two habitats (Pujol and Vergnaud-Grazzini, 1995). This would cause similar levels of 'noise' in the $\delta^{18}\text{O}$ record as the inferred spring habitat, and we conclude that there would be little hope to better constrain the palaeohabitat of species with such bi-(or multi-)modal abundance distributions.

Orbulina universa and both morphotypes of *Globigerinoides sacculifer* today appear as typical

summer mixed-layer dwellers (Pujol and Vergnaud-Grazzini, 1995). The isotope reconstructions for S5 and S1 presented here suggest similar behaviour in the past. In other areas, these species show a tendency to secrete part of the shell at deeper levels within the summer mixed layer

(e.g. Hemleben et al., 1989; Bijma and Hemleben, 1994), which would agree with our observation that they recorded much less of the freshwater dilution at S5 times than *Globigerinoides ruber* (w). *Globigerinita glutinata*'s modern habitat in the Mediterranean was not well resolved, but a

Table 5
Comparison of modern observations with palaeohabitats inferred in the present study

	Summary of modern habitat preferences within Mediterranean ^a	Additional observations outside Mediterranean	Inferred Mediterranean habitat during S5 ^b	Agreement Yes/No
<i>G. ruber</i> (white)	Upper 50 m (summer), less abundant also in upper 100 m (winter) ^c .	Associated with freshwater dilution in Atlantic/Caribbean ^d	S.ml+lenses	Y
<i>G. ruber</i> (pink)	Very shallow (~20 m), with possible second peak just above summer thermocline ^c		Spring or bimodal?	N?
<i>G. sacculifer</i>	Not many found, but together with <i>trilobus</i> types ^c		S.ml	Y
<i>G. sacculifer</i> (<i>trilobus</i> type)	Summer mixed layer (20–50 m) ^c		S.ml	Y
<i>O. universona</i>	Summer mixed layer (to thermocline) ^c	Summer mixed layer down to thermocline ^d	S.ml	Y
<i>G. glutinata</i>	Rare, in winter conditions and to depths of 200 m (Mediterranean campaigns did not sample spring) ^c .	North Atlantic: spring and fall dominance to considerable depth (~200 m) ^e .	Spring	Y
<i>G. bulloides</i>	Mainly winter and early spring. Great depth range, from very shallow to mesopelagic ^c		Spring	~Y
<i>G. siphonifera</i>	Winter mixed layer, peaks at considerable depth ^c		Winter ml	Y
<i>N. pachyderma</i> (dextral)	Year-round, mesopelagic (50–200 m) ^c . Linked to density stratification and Deep Chlorophyll Maximum ^{f,g}		Ssth/Int	Y
<i>G. scitula</i>	Not known from the Mediterranean.	Lives deep in North Atlantic and Caribbean (> 100 m) ^{d,e}	(Ssth)/Int	Y
<i>G. inflata</i>	Mainly winter, but year-round at frontal settings ^{c,f}		Winter ml ^h	Y

^a Summary of modern Mediterranean habitat observations based on late summer and winter plankton tows by Pujol and Vergnaud-Grazzini (1995) for entire Mediterranean. For species reported from the eastern Mediterranean specifically, most weight is given to their habitat descriptions in that basin. Where additional observations from other studies are included, the relevant reference is indicated with superscript numbering.

^b Abbreviations: S.ml., summer mixed layer; Spring, spring bloom conditions; Winter ml., winter mixed layer; Ssth, summer subthermocline waters; Int., intermediate water; Sml+lenses, summer mixed layer with affinity for freshwater diluted conditions.

^c Pujol and Vergnaud-Grazzini (1995)

^d Schmuker, 2000; Schiebel et al. (2002)

^e Schiebel and Hemleben, 2000

^f Rohling et al. (1995)

^g Rohling and Gieskes (1989)

^h Derived in this study from the Late Glacial to Holocene record in core LC21 (Fig. 12).

main preference for spring, as inferred here, would not be incompatible with its very low abundances in the summer and winter tows. The same holds true for *Globigerina bulloides*, for which Pujol and Vergnaud-Grazzini (1995) actually report peak abundances in spring in the Alboran Sea (westernmost Mediterranean). *Hastigerina pelagica* remains enigmatic, and no definite conclusions can be formulated on the basis of its sparse occurrences. *Globigerinella siphonifera* today appears to be a winter mixed-layer species, which agrees with our reconstruction of its habitat during deposition of S5. The modern abundance distribution of *Neogloboquadrina pachyderma* (d) is complex, as there seems to be no strict seasonal preference. In the Mediterranean today, it is a mesopelagic species, associated with density/nutrient gradients at depth (Pujol and Vergnaud-Grazzini, 1995; Rohling et al., 1995), which agrees with the isotopic results for both S5 and S1 presented here. The mesopelagic habitat of *Globorotalia scitula* inferred from the stable isotope study in this paper cannot be compared with the present, since no living *G. scitula* have yet been observed in the Mediterranean basin, while it is also absent from core-top samples. The habitat reconstruction for *Globorotalia inflata* during S1 deposition is compatible with its modern preferences as well.

Table 5 summarises the inferred palaeohabitats for the various species investigated within especially S5 and also S1, in comparison with modern observations. It is apparent that there is a broad agreement between modern and inferred (S5-time) palaeohabitats, which is reassuring for the purposes of environmental reconstructions based on shell chemistry. However, some species, such as *Globigerinoides ruber* (w), do not appear to show their full environmental range in the Mediterranean today, but can adapt to anomalies such as excess freshwater input in accordance with their observed preferences/tolerances outside the Mediterranean. This observation offers a strong argument that detailed shell-chemistry work should rely on reconstruction methods such as presented here to diagnose palaeohabitats, rather than infer them simply in terms of the niches occupied today.

5. Concluding remarks

Whole-faunal stable isotope studies elucidate which species in a specific study interval/area are best to assess overall changes in the climatic/hydrographic state of a basin, including depth-related differentiations and the main seasonal developments, and which species in contrast were most affected by variable biological controls or local/regional and transient physico-chemical forcings. Even when performed within a whole-fauna context, palaeoenvironmental interpretations based on multiple-specimen shell chemistry will be limited by the fact that the observed signals represent multi-annual weighted averages of a wide range of possible peak shell-production seasons, the relative importances of which may shift through the annual cycle in a species-specific manner (shell chemistry depends as much on biology as on physico-chemical conditions). A single-shell analytical approach seems essential before any biologically constrained habitat shifting, and/or the impact of transient features, can be addressed in earnest. Impacts of transient features and/or biological controls on habitat may result in signal amplitudes that rival those of the ‘general’ underlying trends, and – if overlooked – would seriously bias the palaeoenvironmental reconstructions. The present study finds that, at times of sapropel deposition, *Globigerinoides ruber* (w) records tend to be compromised by concentrated signals from such a transient feature, namely freshwater-diluted lenses. Application of this species’ isotope ratios to characterise the ‘main state’ of the basin will severely overestimate the magnitude of the freshwater influx. In other settings, one could envisage that transient eddies act as foci of shell production, which would bias shell-chemistry-based reconstructions since temperature, nutrient, and salinity distributions in transient eddies generally differ from those in ambient waters.

Once the nature of the faunal responses (here in the Mediterranean) to a particular type of environmental perturbation (here enhanced freshwater influx) is understood, intensity differences between different sites or events can be evaluated. Our three records through S5 show considerable sim-

ilarities – suggesting a general change in the basin-wide conditions – as well as distinct local/regional differences in the signal responses and intensities that are related to superimposed local/regional influences. We also find great similarities between the signals through sapropels S5 and S1, although the intensities of change are considerably higher in S5.

Although labour intensive and analytically expensive, a quantitatively interpreted full-faunal stable-isotope data set offers crucial advances in the understanding of temporal changes, differences between separate events, and spatial contrasts for individual events. The thus diagnosed (rather than ‘imposed’) past habitat structures may be used to target further shell chemistry investigations that focus on specific reconstructions such as vertical property gradients. We also suggest that, to eliminate bias originating from the statistical nature of the specimen selection for analysis, shell-chemistry techniques should strive towards multiple-replicate single-shell analyses per species per sample. These underlying principles apply to all palaeoceanographic problems, not just those concerning Mediterranean sapropels.

Acknowledgements

We thank A. Almogi-Labin, W. Broecker, J. Erez, G. Ganssen, C. Hemleben, A. Kemp, M. Kucera, J. McManus, M. Palmer, G. Schmiedl, A. Scrivner, H. Spero, J. Thomson, D. Vance, and P. Wilson for stimulating discussions, feedback, and suggestions on various aspects of this study. M. Cooper kindly performed the foraminiferal Mg/Ca analyses. This paper contributes to NERC projects NER/B/S/2000/00288 and NER/B/S/2002/00268, and Leverhulme project F/07537/I.

References

Adamson, D.A., Gasse, F., Street, F.A., Williams, M.A.J., 1980. Late Quaternary history of the Nile. *Nature* 288, 50–55.

Bar-Matthews, M., Ayalon, A., Kaufman, A., 2000. Timing

and hydrological conditions of Sapropel events in the Eastern Mediterranean, as evident from speleothems, Soreq cave, Israel. *Chem. Geol.* 169, 145–156.

Bauch, D.J.C., Wefer, G., 1997. Oxygen isotope composition of living *Neogloboquadrina pachyderma* (s) in the Arctic ocean. *Earth Planet. Sci. Lett.* 146, 47–58.

Bé, A.W.H., Bishop, J.K.B., Sverdrlove, M.S., Gardner, W.D., 1985. Standing stock, vertical distribution and flux of planktonic foraminifera in Panama Basin. *Mar. Micropaleontol.* 9, 307–333.

Bemis, B.E., Spero, H.J., Bijma, J., Lea, D.W., 1998. Re-evaluation of the oxygen composition of planktonic foraminifera: Experimental results and revised paleotemperature equations. *Paleoceanography* 13, 150–160.

Bijma, J., Hemleben, C., 1994. Population dynamics of the planktic foraminifer *Globigerinoides sacculifer* (Brady) from the central Red Sea. *Deep-Sea Res.* I 41, 485–510.

Bouvier-Soumagnac, Y., Duplessy, J.C., 1985. Carbon and oxygen isotopic composition of planktonic foraminifera from laboratory culture, plankton tows and recent sediment: Implications for the reconstruction of paleoclimatic conditions and of the global carbon cycle. *J. Foraminif. Res.* 15, 302–320.

Boyle, E.A., Keigwin, L., 1982. Deep circulation of the North Atlantic over the last 200,000 years: Geochemical evidence. *Science* 218, 784–787.

Boyle, E.A., Keigwin, L., 1985. Comparison of Atlantic and Pacific paleochemical records for the last 215,000 years: Changes in deep ocean circulation and chemical inventories. *Earth Planet. Sci. Lett.* 76, 135–150.

Boyle, E.A., Keigwin, L., 1987. North Atlantic thermohaline circulation during the past 20,000 years linked to high-latitude surface temperatures. *Nature* 330, 35–40.

Bryden, H.L., Kinder, T.H., 1991. Steady two-layer exchange through the Strait of Gibraltar. *Deep-Sea Res.* I 38, S445–S463.

Calef, G.W., Grice, G.D., 1967. Influence of the Amazon River outflow on the ecology of the western Tropical Atlantic, II. Zooplankton abundance, copepod distribution, with remarks on the fauna of low-salinity areas. *J. Mar. Res.* 25, 84.

Cane, T., Rohling, E.J., Kemp, A.E.S., Cooke, S., Pearce, R.B., 2002. High-resolution stratigraphic framework for Mediterranean sapropel S5: Defining temporal relationships between records of Eemian climate variability. *Palaeogeogr. Palaeoclimatol. Palaeoecol.* 183, 87–101.

Casford, J.S.L., Abu-Zied, R., Rohling, E.J., Cooke, S., Boesenskool, K.P., Brinkhuis, H., De Vries, C., Wefer, G., Gerga, M., Papatheodorou, G., Croudace, I., Thomson, J., Wells, N.C., Lykousis, V., 2001. Mediterranean climate variability during the Holocene. *Mediterr. Mar. Sci.* 2, 45–55.

Casford, J.S.L., Rohling, E.J., Abu-Zied, R., Cooke, S., Fontanier, C., Leng, M., Lykousis, V., 2002. Circulation changes and nutrient concentrations in the Late Quaternary Aegean Sea: A non-steady state concept for sapropel formation. *Paleoceanography* 17, 0.1029/2000PA000601.

Casford, J.S.L., Rohling, E.J., Abu-Zied, R.H., Jorissen, F.J.,

- Leng, M., Thomson, J., 2003. A dynamic concept for eastern Mediterranean circulation and oxygenation during sapropel formation. *Palaeogeogr. Palaeoclimatol. Palaeoecol.* 190, 103–119.
- Castradori, D., 1993. Calcareous nannofossils and the origin of eastern Mediterranean sapropels. *Paleoceanography* 8, 459–471.
- Coplen, T.B., Kendall, C., Hoppole, J., 1983. Comparison of stable isotope reference samples. *Nature* 302, 236–238.
- Corselli, C., Principato, M.S., Maffioli, P., Crudeli, D., 2002. Changes in planktonic assemblages during sapropel S5 deposition: Evidence from Urania Basin area, eastern Mediterranean. *Paleoceanography* 17, 1.1–1.30 (10.1029/2000PA000536).
- Cramp, A., O'Sullivan, G., 1999. Neogene sapropels in the Mediterranean: A review. *Mar. Geol.* 153, 11–28.
- Darling, K.F., Wade, C.M., Stewart, I.A., Kroon, D., Dingle, R., Brown, A.J.L., 2000. Molecular evidence for genetic mixing of Arctic and Antarctic subpolar populations of planktonic foraminifers. *Nature* 405, 43–47.
- De Lange, G.J., Middelburg, J.J., Van der Weijden, C.H., Catalano, G., Luther III, G.W., Hydes, D.J., Woitiez, J.R.W., Klinkhammer, G.P., 1990. Composition of anoxic hypersaline brines in the Tyro and Bannock Basin, eastern Mediterranean. *Mar. Chem.* 31, 63–88.
- De Rijk, S., Rohling, E.J., Hayes, A., 1999. Onset of climatic deterioration in the eastern Mediterranean around 7 ky BP: Micropalaeontological data from Mediterranean sapropel interruptions. *Mar. Geol.* 153, 337–343.
- Deuser, W.G., Ross, E.H., 1989. Seasonally abundant planktonic foraminifera of the Sargasso Sea: Succession, deep-water fluxes, isotopic compositions, and paleoceanographic implications. *J. Foraminif. Res.* 19, 268–293.
- Duplessy, J.C., Labeyrie, L., Juillet-Leclerc, A., Maître, F., Duprat, J., Sarnthein, M., 1991. Surface salinity reconstruction of the North Atlantic Ocean during the last glacial maximum. *Oceanol. Acta* 14, 311–324.
- Emeis, K.-C., Schulz, H.-M., Struck, U., Sakamoto, T., Doose, H., Erlenkeuser, H., Howell, M., Kroon, D., Paterne, M., 1998. Stable isotope and temperature records of sapropels from ODP Sites 964 and 967: Constraining the physical environment of sapropel formation in the Eastern Mediterranean Sea. In: Robertson, A.H.F., Emeis, K.-C., Richter, C., Camerlenghi, A. (Eds.), *Proc. ODP, Sci. Res.* 160. Ocean Drilling Program, College Station, TX, pp. 309–331.
- Emeis, K.-C., Struck, U., Schulz, H.-M., Bernasconi, S., Sakamoto, T., Martinez-Ruiz, F., 2000. Temperature and salinity of Mediterranean Sea surface waters over the last 16,000 years: Constraints on the physical environment of S1 sapropel formation based on stable oxygen isotopes and alkenone unsaturation ratios. *Palaeogeogr. Palaeoclimatol. Palaeoecol.* 158, 259–280.
- Emeis, K.-C., Schulz, H., Struck, U., Rossignol-Struck, M., Erlenkeuser, H., Howell, M.W., Kroon, D., Mackensen, H., Ishizuka, S., Oba, T., Sakamoto, T., Koizumi, I., 2003. Eastern Mediterranean surface water temperatures and $\delta^{18}\text{O}$ composition during deposition of sapropels in the late Quaternary. *Paleoceanography* 18, 10.1029/2000PA000617.
- Fairbanks, R.G., Sverdrlove, M., Free, R., Wiebe, P.H., Bé, A.W.H., 1982. Vertical distribution of living planktonic foraminifera from the Panama Basin. *Nature* 298, 841–844.
- Fontugne, M.R., Calvert, S.E., 1992. Late Pleistocene variability of the organic carbon isotopic composition of organic matter in the eastern Mediterranean: Monitor of changes in organic carbon sources and atmospheric CO_2 concentrations. *Paleoceanography* 7, 1–20.
- Fontugne, M., Arnold, M., Labeyrie, L., Paterne, M., Calvert, S., Duplessy, J.C., 1994. Paleoenvironment, sapropel chronology, and Nile river discharge during the last 20,000 years as indicated by deep-sea sediment records in the eastern Mediterranean. *Radiocarbon* 34, 75–88.
- Ganssen, G., Troelstra, S.R., 1987. Paleoenvironmental changes from stable isotopes in planktonic foraminifera from Eastern Mediterranean sapropels. *Mar. Geol.* 75, 221–230.
- Garrett, C., Outerbridge, R., Thompson, K., 1993. Inter-annual variability in Mediterranean heat budget and buoyancy fluxes. *J. Climatol.* 6, 900–910.
- Gasse, F., 2000. Hydrological changes in the African tropics since the last glacial maximum. *Quat. Sci. Rev.* 19, 189–211.
- Grossman, E.L., 1987. Stable isotopes in modern benthic foraminifera: A study of vital effect. *J. Foraminif. Res.* 17, 48–61.
- Hassan, F.A., 1997. The dynamics of a riverine civilization: A geoarchaeological perspective on the Nile Valley, Egypt. *World Archaeol.* 29, 51–74.
- Hayes, A., Kucera, M., Rohling, E., Kallel, N., 2003. Foraminifer assemblage-based SST reconstruction using Artificial Neural Networks records distinct cooling events associated with the Mediterranean Holocene sapropel. *Geophysical Research Abstracts* 5 (CD-ROM), EGS–EUG–AGU 28th Assembly, Nice, Abstract P1393.
- Hemleben, C., Meischner, D., Zahn, R., Almogi-Labin, A., Erlenkeuser, H., Hiller, B., 1996. Three hundred eighty thousand year long stable isotope and faunal records from the Red Sea: Influence of global sea level change on hydrography. *Paleoceanography* 11, 147–156.
- Hemleben, C., Spindler, M., Anderson, O.R., 1989. *Modern Planktonic Foraminifera*. Springer, New York, 363 pp.
- Hemleben, Ch., Spindler, M., 1983. Recent advances in research on living planktonic foraminifera: Reconstruction of marine paleoenvironments. *Utrecht Micropaleontological Bulletin* 30, 141–170.
- Hoelzmann, P., Kruse, H.J., Rottinger, F., 2000. Precipitation estimates for the eastern Saharan palaeomonsoon based on a water balance model of the West Nubian palaeolake basin. *Glob. Planet. Change* 26, 105–120.
- Jenkins, J.A., Williams, D.F., 1984. Nile water as a cause of eastern Mediterranean sapropel formation: Evidence for and against. *Mar. Micropaleontol.* 9, 521–534.
- Jorissen, F.J., Asioli, A., Borsetti, A.M., Capotondi, L., De Visscher, J.P., Hilgen, F.J., Rohling, E.J., Van der Borg, K., Vergnaud-Grazzini, C., Zachariasse, W.J., 1993. Late Qua-

- ternary central Mediterranean biochronology. *Mar. Micropaleontol.* 21, 169–189.
- Kallel, N., Paterne, M., Duplessy, J.C., Vergnaud-Grazzini, C., Pujol, C., Labeyrie, L., Arnold, M., Fontugne, M., Pierre, C., 1997a. Enhanced rainfall in the Mediterranean region during the last sapropel event. *Oceanol. Acta* 20, 697–712.
- Kallel, N., Paterne, M., Labeyrie, L., Duplessy, J.C., Arnold, M., 1997b. Temperature and salinity records of the Tyrrhenian Sea during the last 18,000 years. *Palaeogeogr. Palaeoclimatol. Palaeoecol.* 135, 97–108.
- Kim, S.T., O'Neil, J.R., 1997. Equilibrium and nonequilibrium oxygen isotope effects in synthetic calcites. *Geochim. Cosmochim. Acta* 61, 3461–3475.
- Kucera, M., Darling, K.F., 2002. Cryptic species of planktonic foraminifera: Their effect on palaeoceanographic reconstructions. *Philos. Trans. R. Soc. Lond. A* 360, 695–718.
- Labeyrie, L., Labracherie, M., Gorfti, N., Pichon, J.J., Vautravers, M., Arnold, M., Duplessy, J.C., Paterne, M., Michel, E., Duprat, J., Caralp, M., Turon, J.L., 1996. Hydrographic changes of the Southern ocean (southeast Indian sector) over the last 230 kyr. *Paleoceanography* 11, 57–76.
- Maslin, M.A., Shackleton, N.J., Pflaumann, U., 1995. Surface water temperature, salinity, and density changes in the northeast Atlantic during the last 45,000 years: Heinrich events, deep water formation, and climatic rebounds. *Paleoceanography* 10, 527–544.
- Maynard, K., Royer, J.F., Chauvin, F., 2002. Impact of greenhouse warming on the west African summer monsoon. *Climate Dynamics* (on-line number 10.1007/s00382-002-0242-z).
- McKenzie, J.A., 1993. Pluvial conditions in the eastern Sahara following the penultimate deglaciation: Implications for changes in atmospheric circulation patterns with global warming. *Palaeogeogr. Palaeoclimatol. Palaeoecol.* 103, 95–105.
- Mercione, D., Thomson, J., Croudace, I.W., Siani, G., Paterne, M., Troelstra, S., 2000. Duration of S1, the most recent sapropel in the eastern Mediterranean Sea, as indicated by accelerator mass spectrometry radiocarbon and geochemical evidence. *Paleoceanography* 15, 336–347.
- Mercione, D., Thomson, J., Abu-Zied, R.H., Croudace, I.W., Rohling, E.J., 2001. High-resolution geochemical and micro-palaeontological profiling of the most recent eastern Mediterranean sapropel. *Mar. Geol.* 177, 25–44.
- Mielke, K.M., 2001. Reconstructing Surface Carbonate Chemistry and Temperature in Palaeoceans: Geochemical Results from Laboratory Experiments and the Fossil Record. M.Sc. Thesis, University California at Davis, Davis, CA, 166 pp.
- Müller, P.J., Kirst, G., Ruhland, G., von Storch, I., Rosell-Mélé, A., 1998. Calibration of the alkenone paleotemperature index UK'37 based on core tops from the eastern South Atlantic and the global ocean (60°N–60°S). *Geochim. Cosmochim. Acta* 62, 1757–1772.
- Murat, A., 1984. Sequences et paléoenvironnements marins Quaternaires. Une marge active: l'arc Hellenique oriental. Ph.D. Thesis (3rd cycle), Univ. of Perpignan, 280 pp.
- Myers, P.G., Hayes, K., Rohling, E.J., 1998. Modelling the paleo-circulation of the Mediterranean: The Last Glacial Maximum and the Holocene with emphasis on the formation of sapropel S1. *Paleoceanography* 13, 586–606.
- Myers, P.G., Rohling, E.J., 2000. Modelling a 200 year interruption of the Holocene sapropel S1. *Quat. Res.* 53, 98–104.
- National Institute of Standards and Technology, 1992. Report of Investigation, Reference Materials, pp. 8543–8546.
- Nof, D., 1981. On the dynamics of equatorial outflows with application to the Amazon's basin. *J. Mar. Res.* 39, 1–29.
- O'Neil, J.R., Clayton, R.N., Mayeda, T.K., 1969. Oxygen isotope fractionation on divalent metal carbonates. *J. Chem. Phys.* 51, 5547–5558.
- Ortiz, J.D., Mix, A.C., Rugh, W., Watkins, J.M., Collier, R.W., 1996. Deep-dwelling planktonic foraminifera of the northeastern Pacific Ocean reveal environmental control of oxygen and carbon isotope disequilibria. *Geochim. Cosmochim. Acta* 60, 4509–4523.
- Palmer, M.R., Pearson, P.N., Cobb, S.J., 1998. Reconstructing past ocean pH-depth profiles. *Science* 282, 1468–1471.
- Parisi, E., 1987. Carbon and Oxygen isotope composition of Globorinoides ruber in two deep sea cores from the Levantine Basin (eastern Mediterranean). *Mar. Geol.* 75, 201–219.
- Pawlowski, J., Holzmann, M., 2002. Molecular phylogeny of Foraminifera – a review. *Eur. J. Protistol.* 38, 1–10.
- Pearson, P.N., Palmer, M.R., 1999. Middle Eocene seawater pH and atmospheric carbon dioxide concentrations. *Science* 284, 1824–1826.
- Pearson, P.N., Palmer, M.R., 2000. Estimating Paleogene atmospheric pCO₂ using boron isotope analysis of foraminifera. *GFF* 122, 127–128.
- Peeters, F., 2000. The distribution and stable isotope composition of living planktic foraminifera in relation to seasonal changes in the Arabian Sea. Ph.D. Thesis, Free University Amsterdam, 184 pp.
- Pierre, C., 1999. The oxygen and carbon isotope distribution in the Mediterranean water masses. *Mar. Geol.* 153, 41–55.
- POEM group, 1992. General circulation of the eastern Mediterranean. *Earth-Sci. Rev.* 32, 285–309.
- Pujol, C., Vergnaud-Grazzini, C., 1989. Palaeoceanography of the last deglaciation in the Alboran Sea (western Mediterranean): Stable isotopes and planktonic foraminiferal records. *Mar. Micropaleontol.* 15, 153–179.
- Pujol, C., Vergnaud-Grazzini, C., 1995. Distribution patterns of live planktic foraminifera as related to regional hydrography and productive systems of the Mediterranean Sea. *Mar. Micropaleontol.* 25, 187–217.
- Ravelo, A.C., Fairbanks, R.G., 1995. Carbon isotopic fractionation in multiple species of planktonic foraminifera from core-tops in the tropical Pacific. *J. Foraminif. Res.* 25, 53–74.
- Reiss, Z., Halicz, E., Luz, B., 1999. Late-Holocene foraminifera from the SE Levantine Basin. *Isr. J. Earth Sci.* 48, 1–17.
- Reynolds, L.A., Thunell, R.C., 1989. Seasonal succession of planktonic foraminifera: Results from a four-year time-series sediment trap experiment in the northeast Pacific. *J. Foraminif. Res.* 19, 253–267.

- Roether, W., Well, R., 2001. Oxygen consumption in the eastern Mediterranean. *Deep-Sea Res. I* 48, 1535–1551.
- Rohling, E.J., 1994. Review and new aspects concerning the formation of Mediterranean sapropels. *Mar. Geol.* 122, 1–28.
- Rohling, E.J., 1999. Environmental controls on salinity and $\delta^{18}\text{O}$ in the Mediterranean. *Paleoceanography* 14, 706–715.
- Rohling, E.J., 2000. Paleosalinity: Confidence limits and future applications. *Mar. Geol.* 163, 1–11.
- Rohling, E.J., Bigg, G.R., 1998. Paleosalinity and $\delta^{18}\text{O}$: A critical assessment. *J. Geophys. Res.* 103, 1307–1318.
- Rohling, E.J., Cooke, S., 1999. Stable oxygen and carbon isotope ratios in foraminiferal carbonate. In: Sen Gupta, B.K. (Ed.), *Modern Foraminifera*. Kluwer Academic, Dordrecht, pp. 239–258.
- Rohling, E.J., De Rijk, S., 1999. The Holocene Climate Optimum and Last Glacial Maximum in the Mediterranean: The marine oxygen isotope record. *Mar. Geol.* 153, 57–75.
- Rohling, E.J., Gieskes, W.W.C., 1989. Late Quaternary changes in Mediterranean Intermediate Water density and formation rate. *Paleoceanography* 4, 531–545.
- Rohling, E.J., Hilgen, F.J., 1991. The eastern Mediterranean climate at times of sapropel formation: A review. *Geol. Mijnb.* 70, 253–264.
- Rohling, E.J., Cane, T.R., Cooke, S., Sprovieri, M., Bouloubassi, I., Emeis, K.C., Schiebel, R., Kroon, D., Jorissen, F.J., Lorre, A., Kemp, A.E.S., 2002. African monsoon variability during the previous interglacial maximum. *Earth Planet. Sci. Lett.* 202, 61–75.
- Rohling, E.J., De Rijk, S., Myers, P., Haines, K., 2000. Traditional palaeoceanography and numerical modelling: The Mediterranean Sea at times of sapropel formation. In: Hart, M.B. (Ed.), *Climates: Past and Present*. Geol. Soc. Spec. Publ. 181, pp. 135–149.
- Rohling, E.J., Den Dulk, M., Pujol, C., Vergnaud-Grazzini, C., 1995. Abrupt hydrographic change in the Alboran Sea (western Mediterranean) around 8000 yrs BP. *Deep-Sea Res.* 42, 1609–1619.
- Rohling, E.J., Jorissen, F.J., Vergnaud-Grazzini, C., Zachariasse, W.J., 1993. Northern Levantine and Adriatic Quaternary planktic foraminifera: Reconstruction of paleoenvironmental gradients. *Mar. Micropaleontol.* 21, 191–218.
- Rosignol-Strick, M., 1983. African monsoons, an immediate climatic response to orbital insolation. *Nature* 304, 46–49.
- Rosignol-Strick, M., 1985. Mediterranean Quaternary sapropels, an immediate response to the African monsoon to variation of insolation. *Palaeogeogr. Palaeoclimatol. Palaeoecol.* 49, 237–263.
- Rosignol-Strick, M., 1987. Rainy periods and bottom water stagnation initiating brine concentrations, 1. The late Quaternary. *Paleoceanography* 2, 330–360.
- Rosignol-Strick, M., Nesteroff, W., Olive, P., Vergnaud-Grazzini, C., 1982. After the deluge: Mediterranean stagnation and sapropel formation. *Nature* 295, 105–110.
- Rostek, F., Ruhland, G., Bassinot, F.C., Müller, P.J., Labeyrie, L., Lancelot, Y., Bard, E., 1993. Reconstructing sea surface temperature and salinity using $\delta^{18}\text{O}$ and alkenone records. *Nature* 364, 319–321.
- Rozanski, K., 1985. Deuterium and oxygen-18 in European groundwaters – links to atmospheric circulation in the past. *Chem. Geol. (Isot. Geosci. Sect.)* 52, 349–363.
- Ryther, J.H., Menzel, D.W., Corwin, N., 1967. Influence of the Amazon River outflow on the ecology of the western tropical Atlantic, I. Hydrography and nutrient chemistry. *J. Mar. Res.* 25, 69–83.
- Schiebel, R., Hemleben, Ch., 2000. Interannual variability of planktic foraminiferal populations and test flux in the eastern North Atlantic Ocean (JGOFS). *Deep-Sea Res. II* 47, 1809–1852.
- Schiebel, R., Waniek, J., Bork, M., Hemleben, Ch., 2001. Planktic foraminiferal production stimulated by chlorophyll redistribution and entrainment of nutrients. *Deep-Sea Res. I* 48, 721–740.
- Schiebel, R., Waniek, J., Zeltner, A., Alves, M., 2002. Impact of the Azores Front on the distribution of planktic foraminifers, shelled gastropods, and coccolithophorids. *Deep-Sea Res. II* 49, 4035–4050.
- Schmidt, G.A., 1999a. Error analysis of paleosalinity calculations. *Paleoceanography* 14, 422–429.
- Schmidt, G.A., 1999b. Forward modelling of carbonate proxy data from planktic foraminifera using oxygen isotope tracers in a global ocean model. *Paleoceanography* 14, 482–497.
- Schmuker, B., 2000. Recent Planktic Foraminifera in the Caribbean Sea: Distribution, Ecology and Taphonomy, Ph.D. Thesis, ETH, Zürich, 167 pp.
- Schmuker, B., Schiebel, R., 2002. Planktic foraminifers and hydrography of the eastern and northern Caribbean Sea. *Mar. Micropaleontol.* 46, 387–403.
- Simstich, J., Sarnthein, M., Erlenkeuser, H., 2003. Paired $\delta^{18}\text{O}$ signals of *Neogloboquadrina pachyderma* (s) and *Turborotalita quinqueloba* show thermal stratification structure in Nordic Seas. *Mar. Micropaleontol.* 48, 107–125.
- Sonntag, C., Klitzsch, E., Löhnert, E.P., El Shazly, E.M., Münnich, K.O., Junghans, Ch., Thorweihe, U., Weistroffer, K., Swailem, F.M., 1979. Paleoclimatic information from deuterium and oxygen-18 in carbon-14-dated north Saharan groundwaters. In: *Isotope Hydrology 1978, II*. Int. At. Energy Agency, Vienna, pp. 569–580.
- Spero, H.J., 1992. Do planktic foraminifera accurately record shifts in the carbon isotopic composition of sea water ΣCO_2 ? *Mar. Micropaleontol.* 19, 275–285.
- Spero, H.J., Lea, D.W., 1993. Intraspecific stable isotope variability in the planktic foraminifera *Globigerinoides sacculifer*: Results from laboratory experiments. *Mar. Micropaleontol.* 22, 221–234.
- Spero, H.J., Williams, D.F., 1988. Extracting environmental information from planktic foraminiferal $\delta^{13}\text{C}$ data. *Nature* 335, 717–719.
- Spero, H.J., Lerche, I., Williams, D.F., 1991. Opening the carbon isotope ‘vital effect’ black box, 2, quantitative model for interpreting foraminiferal carbon isotope data. *Paleoceanography* 6, 639–655.

- Spero, H.J., Mielke, K.M., Kalve, E.M., Lea, D.W., Pak, D.K., 2003. Multi-species approach to reconstructing Eastern Equatorial Pacific thermocline hydrography during the past 360 ky. *Paleoceanography*, 18, 10.1029/2002PA000814.
- Stanev, E.V., Friedrich, H.J., Botev, S.V., 1989. On the seasonal response of intermediate and deep water to surface forcing in the Mediterranean Sea. *Oceanol. Acta* 12, 141–149.
- Stanley, D.J., Maldonado, A., 1979. Levantine Sea–Nile Cone lithostratigraphic evolution: Quantitative analysis and correlation with paleoclimatic and eustatic oscillations in the Late Quaternary. *Sediment. Geol.* 23, 37–65.
- Stewart, I.A., Darling, K.F., Kroon, D., Wade, C.M., Troelstra, S.R., 2001. Genotypic variability in subarctic Atlantic planktic foraminifera. *Mar. Micropaleontol.* 43, 143–153.
- Struck, U., Emeis, K.C., Voss, M., Krom, M.D., Rau, G.H., 2001. Biological productivity during sapropel S5 formation in the Eastern Mediterranean Sea: Evidence from stable isotopes of nitrogen and carbon. *Geochim. Cosmochim. Acta* 65, 3249–3266.
- Tang, C.M., Stott, L.D., 1993. Seasonal salinity changes during Mediterranean sapropel deposition 9000 years B.P.: Evidence from isotopic analyses of individual planktonic foraminifera. *Paleoceanography* 8, 473–493.
- Thomson, J., Higgs, N.C., Wilson, T.R.S., Croudace, I.W., De Lange, G.J., Van Santvoort, P.J.M., 1995. Redistribution and geochemical behaviour of redox-sensitive elements around S1, the most recent eastern Mediterranean sapropel. *Geochim. Cosmochim. Acta* 59, 3487–3501.
- Thunell, R.C., Reynolds, L.A., 1984. Sedimentation of planktonic foraminifera: Seasonal changes in species flux in the Panama Basin. *Micropaleontology* 30, 243–262.
- Thunell, R.C., 1978. Distribution of recent planktonic foraminifera in surface sediments of the Mediterranean Sea. *Mar. Micropaleontol.* 3, 147–173.
- Thunell, R.C., Williams, D.F., 1989. Glacial–Holocene salinity changes in the Mediterranean Sea: Hydrographic and depositional effects. *Nature* 338, 493–496.
- Troelstra, S.R., Ganssen, G.M., Van der Borg, K., De Jong, A.F.M., 1991. A Late Quaternary stratigraphic framework for eastern Mediterranean sapropel S1 based on AMS 14C dates and stable isotopes. *Radiocarbon* 33, 15–21.
- Ufkes, E., Jansen, J.H.F., Brummer, G.J.A., 1998. Living planktonic foraminifera in the eastern South Atlantic during spring: Indicators of water masses, upwelling, and the Congo (Zaire) River plume. *Mar. Micropaleontol.* 33, 27–53.
- Vergnaud-Grazzini, C., 1985. Mediterranean late Cenozoic stable isotope record: Stratigraphic and paleoclimatic implications. In: Stanley, D.J., Wezel, F.C. (Eds.), *Geological Evolution of the Mediterranean Basin*. Springer, New York, pp. 413–451.
- von Langen, P.J., Lea, D.W., Spero, H.J., 2000. Effects of temperature on oxygen isotope and Mg/Ca values in *Neogloboquadrina pachyderma* shells determined by live culturing. EOS Transactions AGU, Fall mtg. suppl.
- Williams, D.F., Be, A.W.H., Fairbanks, R.G., 1981. Seasonal stable isotopic variations in living planktonic foraminifera from Bermuda plankton tows. *Palaeogeogr. Palaeoclimatol. Palaeoecol.* 33, 71–102.
- Wüst, G., 1961. On the vertical circulation of the Mediterranean Sea. *J. Geophys. Res.* 66, 3261–3271.